Méthodes à faible complexité algorithmique pour l'analyse d'ECG

Ahmad Khoureich Ka

N° d'ordre : ANNÉE 2012

THÈSE / UNIVERSITÉ DE RENNES 1
sous le sceau de l'Université Européenne de Bretagne

pour le grade de

DOCTEUR DE L'UNIVERSITÉ DE RENNES 1

Mention : Traitement du signal et télécommunications

École doctorale Matisse

présentée par

Ahmad Khoureich KA

préparée à l'IRMAR - UMR CNRS 6625
Institut de Recherche Mathématique de Rennes
Université de Rennes 1

Méthodes à faible complexité algorithmique pour l'analyse d'ECG

Thèse soutenue à Rennes le 4 décembre 2012

devant le jury composé de :

Guy CARRAULT
Professeur à l'université de Rennes 1 / président

Corinne MAILHES
Professeur à l'INP de Toulouse / rapporteur

Olivier MESTE
Professeur à l'université de Nice / rapporteur

Dimitri PETRITIS
Professeur à l'université de Rennes 1 / directeur de thèse

Mamadou SANGHARÉ
Professeur à l'université de Dakar / co-directeur de thèse

Méthodes à faible complexité algorithmique pour l'analyse des signaux ECG

Ahmad Khoureich Ka

Remerciements

Mes premiers remerciements vont au Professeur Dimitri Pétritis, pour avoir accepter de m'encadrer pour cette thèse. Je le suis particulièrement reconnaissant pour son soutient, ses conseils, sa patience et sa sagesse. Veuillez accepter, cher Dimitri, l'expression de ma profonde gratitude.

Mes remerciements vont aussi au Professeur Mamadou Sangharé qui a co-encadré ce travail et qui n'a ménagé aucun effort pour l'aboutissement de cette thèse.

Je présente toute ma reconnaissance aux Professeurs Corinne Mailhes et Olivier Meste pour avoir accepter de rapporter sur mon travail et au Professeur Guy Carrault pour avoir accepter de faire partie de mon jury de thèse et de le présider. Croyez Madame, Messieurs, à mon estime et à mon profond respect.

Je remercie les collègues doctorants de l'IRMAR pour avoir manifesté autant d'intérêt à mon égard et m'avoir permis de trouver ma place au sein du groupe. Je pense particulièrement à Jean-Romain Heu, à Thomas Sierocinski et à Mikaël Roger que j'ai connus à ma première année de thèse. Je pense aussi aux collègues de bureau 434 pour leur accueil et leur soutient: Jiaqi Chen, Yoann Offret, Mikaël Roger et Adel Settati.

Je remercie également tout le personnel administratif de l'IRMAR, pour leur écoute, leur gentillesse et leur disponibilité. Je pense particulièrement à Karine Falc'Hon et à Marie-Aude Verger.

Je tiens particulièrement à rendre hommage à mes anciens professeurs qui m'ont toujours soutenu; il s'agit de Dr Ibrahima Niang, de Dr Djiby Sow, Dr Thiecoumba Gueye et de Dr Oumar Djanka. Mes remercements vont aussi à mes collègues et amis de Thies pour leur conseil sur la pratique de la thèse; ce sont les Dr Ibrahima Mbaye et Papa Ibrahima Ndiaye.

Je pense également aux amis de l'Association Culturelle et Sportive des Etudiants Musulmans de Rennes (ACSEMR) que j'ai eu la chance de côtoyer durant mes séjours à Rennes.

Je n'aurai jamais de mots assez chaleureux pour exprimer toute ma gratitude à l'égard des mes parents, mes frères, mes soeurs, à ma femme qui m'a témoigné beaucoup de patience, aussi à mes enfants Fatima et Abdallah qui voulaient tant jouer avec moi alors que j'avais pas assez de temps.

Contents

RÉSUMÉ EN FRANÇAIS

0.1 Introduction

Un électrocardiogramme (ECG) est un enregistrement de l'activité électrique au niveau du cœur. Cette activité électrique est responsable des contractions qui aspirent puis expulsent le sang du cœur et ainsi générer la circulation sanguine dans tout l'organisme. Recueillie à partir d'électrodes placées à la surface de la peau au niveau de la poitrine, cette activité électrique du cœur peut être représentée graphiquement (voir figure 1). L'électrocardiogramme

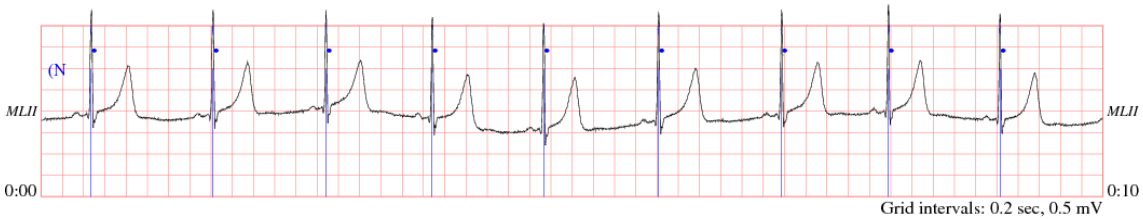

Figure 1: Segment du tracé ECG pris à partir de l'enregistrement 113 du MIT-Arrhythmia Database [23]

est devenu l'un des outils les plus importants dans le diagnostic des maladies de cœur. A partir l'ECG d'un patient, un cardiologue peut analyser la forme des battements cardiaques et diagnostiquer le mal dont il souffre. Il est aussi utilisé comme outil de recherche de potentiels troubles du rythme cardiaque qui pourraient découler de l'utilisation de nouveaux médicaments. Les anomalies dans le fonctionnement du cœur peuvent être rares et disséminées dans un long tracé électrocardiogramme. Par conséquent le travail du cardioloque consistant à traquer ces irrégularités peut être long et fastidieux. Il devenait alors nécessaire d'utiliser des logiciels d'aide au diagnostic. La population de personnes agées vivant seules ou de personnes vivant dans des zones faiblement médicalisées étant en constante croissance, le developpement d'outils de surveillance pouvant détecter en temps réel les irrégularités du cœur et alerter un centre médical proche devient une urgence.

La grande difficulté pour implémenter des solutions logicielles à ces problèmes réside dans la grande variété dans la forme des battements cardiaques de même type (normal ou arythmies) ou de battement de types différents ayant des formes très similaires [1, 3]. C'est pourquoi, les algorithmes des logiciels d'aide au diagnostic ou de surveillance ont généralement trois étapes:

- la localisation des battements cardiaques après le traitement du signal ECG qui est parfois bruité;

- l'extraction d'informations caractéristiques et parfois spécifiques;

- la classification.

Le signal ECG est acquis à l'aide d'électrocardiographe numérique, puis débruité pour augmenter sa qualité. Pour la détection des battements cardiaques, un certain nombre de méthodes sont disponibles dans la littérature [78, 6]. L'extraction d'informations caractéristiques peut se faire dans le domaine temporel (le signal ECG est considéré come une fonction du temps) [13], dans le domaine frequentiel [7], par décomposition multirésolution [9], par analyse multifractale [10] ou par des moyens statistiques [1]. Les méthodes de classifications peuvent être heuristiques [12, 1, 9] ou s'appuyer sur une approche statistique [13, 15].

Bien que les méthodes statistiques de classification donnent de bon pourcentages de reconnaissance de type de battement cardiaque, nous pensons comme Yu Hen Hu [12] qu'une bonne approche pour la classification des battements cardiaques doit tenir compte des spécificités de chaque patient. C'est le cas de la méthode proposée dans cette thèse. La transformation en ondelette a été utilisée avec succès pour le traitement des signaux non stationnaires comme les électrocardiogrammes [11]. Nous l'utiliserons alors pour le débruitage des signaux ECG et pour la compression des battements cardiaques.

Le classificateur proposé utilise une base de données comportant cinq classes de battements. Il a pour but d'identifier 6 types de battements cardiaques dénommés: Normal Beats (NB), Premature Ventricular Contractions (PVC), Paced Beats (PB), Atrial Premature Beat (APB), Left Bundle Branch Block beat (LBBB) and Right Bundle Branch Block beat (RBBB). Dans cette liste à part le type Normal Beat (NB), tous les autres sont des arythmies (troubles du rythme cardiaque). L'exploitation des spécificités de chaque patient pour la classification est mise en œuvre en intégrant les 5 premières minutes de l'ECG annoté de celui-ci dans la base de donnée du classificateur mais aussi en faisant un regroupement (ou clustering) contextuel des battements avant leur identification. Ce qui a aussi comme avantage d'augmenter les "connaissances expérimentales" du classificateur à chaque fois qu'une analyse d'électrocardiogramme est faite. Le classificateur traite dans un premier temps l'électrocardiogramme pour en atténuer le bruit. Ensuite, il extrait les battements cardiaques puis les compresse pour diminuer leur taille (nombres de points). En fin, les battements sont regroupés en cluster en se basant sur la similarité de leur forme. Le type des battements d'un cluster donné correspond au type du battement (contenu dans le cluster) le plus similaire à un battement cardiaque de la base de données.

La méthode de localisation proposée s'appuie sur la décomposition en ondelette pour localiser et identifier les battements normaux. Sur l'ensemble des coefficients d'ondelette obtenus avec la décomposition, seul une partie dénommé **set of parsimony** (composée des coefficients dont la valeur est supérieur à un certain seuil) est utilisée pour la localisation.

Cette méthode commence par marquer les points intéressants du signal ECG, puis utilise une masque pour reconnaitre les potentiels complexe QRS.

Pour la création de la base de données de battements cardiaques connus et l'évaluation des performances du classificateur nous utiliserons 46 enregistrements de la base de données du MIT/BIH arrhythmia database.

0.2 Méthodes de classification et de localisation proposées

0.2.1 Décomposition en ondelettes

Avec l'analyse multirésolution introduite par S. Mallat [45], toute fonction $f \in L^2(\mathbb{R})$ peut être représentée en une série convergente:

$$f(t) = \sum_{k\in\mathbb{Z}} \alpha_{j_0k}\phi_{j_0k}(t) + \sum_{j=j_0}^{\infty}\sum_{k\in\mathbb{Z}} \beta_{jk}\psi_{jk}(t), \tag{1}$$

où

$$\phi_{j_0k}(t) = 2^{j_0/2}\phi(2^j t - k), \quad j_0 \in \mathbb{Z}, k \in \mathbb{Z}$$

avec ϕ étant l'ondelette père et

$$\psi_{jk}(t) = 2^{j/2}\psi(2^j t - k), \quad j \in \mathbb{Z}, k \in \mathbb{Z}$$

ψ étant l'ondelette mère.

Les coefficients α_{j_0k} et β_{jk} sont respectivement les coefficients d'echelles et d'ondelettes.

L'algorithme piramidal de Mallat [49, 50] permet d'obtenir les coefficients d'une résolution inférieure j à partir de ceux de la résolution immédiatement supérieure $j+1$ et vice versa:

$$\alpha_{jk} = \sum_{l\in\mathbb{Z}} h_{l-2k}\alpha_{j+1,l} \quad \text{et} \quad \beta_{jk} = \sum_{l\in\mathbb{Z}} \lambda_{l-2k}\alpha_{j+1,l} \tag{2}$$

$$\alpha_{j+1,l} = \sum_{k} h_{l-2k}\alpha_{jk} + \sum_{k} \lambda_{l-2k}\beta_{jk} \tag{3}$$

où $\lambda_k = (-1)^{k+1}h_{1-k}$ est la réponse impulssionnelle d'un filtre numérique $j \in \mathbb{Z}$ et $k \in \mathbb{Z}$.

0.2.2 Débruitage du signal ECG

Le signal ECG est généralement bruité. Ce bruit se manifeste par l'apparition d'une ligne de base variable et des oscillations rapides à faibles amplitudes (bruit haute fréquence).

Pour l'élimination de la ligne de base variable nous avons utilisé la méthode présentée dans la thèse de A. Khawaja [74]. Pour l'élimination du bruit de haute fréquence la technique de seuillage (soft thresholding) de D. Donoho [75] est utilisée. Nous avons implémenté en

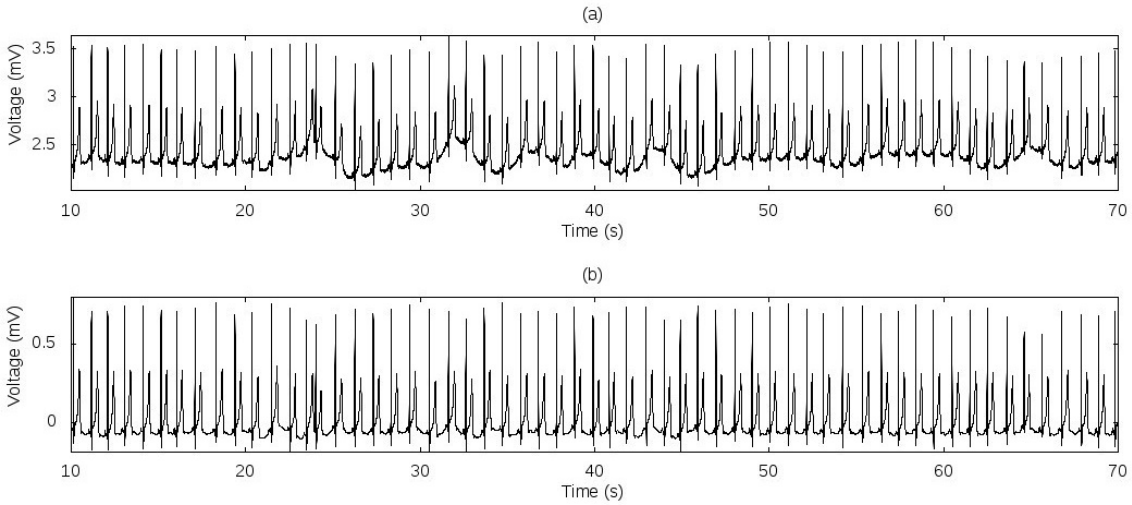

Figure 2: Résultat du débruitage sur un segment du tracé ECG pris à partir de l'enregistrement 113 du MIT-Arrhythmia: (a) Signal original. (b) Signal débruité.

java ces deux techniques de réduction de bruit et l'appliquer à un ECG bruité comme le montre la Figure 0.2.2.

0.2.3 Classification

La morphologie du complexe QRS et l'intervalle RR (voir figure 3) jouent un rôle important dans l'interprétation d'un battement donné [15, 16]. De même la longueur moyenne des intervalles RR situés entre deux battements non prématurés (RR_m) et ratio entre les intervalles RR (RR_{av}) avant un complexe QRS donné et celui qui vient après (RR_{ap}) sont considérés comme informations utiles [17]. Ils sont alors utilisés par le classificateur.

La position des sommets R seront prises à partir des fichiers d'annotations de la base de données du MIT-BIH arrhythmia database. Les battement sont extraits du signal ECG en considérant les 128 points autour de son sommet R. Ils sont ensuite compressés pour réduire leur taille à 16 points à l'aide de l'analyse multirésolution comme suit:

Le battement original de $128 = 2^7$ points est à sa résolution maximale $j_0 = 7$. Son

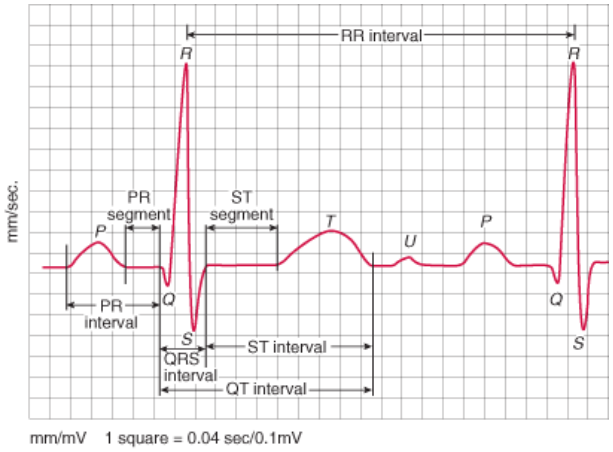

Figure 3: Représentation d'un battement cardiaque normal avec ses différentes composantes. Figure adaptée à partir de [18]

expansion sur la base d'ondelette s'écrit

$$b_{128}(t) = \sum_{k=0}^{2^7-1} \alpha_{7,k}\phi_{7,k}(t), \tag{4}$$

Sa décomposition à un niveau de résolution 3 fois inférieur est

$$b_{128}(t) = \sum_{k=0}^{2^4-1} \alpha_{4,k}\phi_{4,k}(t) + \sum_{j=4}^{7}\sum_{k=0}^{2^j-1} \beta_{jk}\psi_{jk}(t), \tag{5}$$

En annulant les coefficients d'ondellette β_{jk} nous obtenons la forme compressée du battement

$$b_{16}(t) = \sum_{k=0}^{2^4-1} \alpha_{4,k}\phi_{4,k}(t) \tag{6}$$

Ce battement compressé de 16 points est alors considérer comme une information utile pour la classification. L'avantage de cette compression est que le processus de classification est accéléré tout en utilisant moins de ressource mémoire.

L'identification de la classe d'un battement est faite à l'aide de la fonction de similarité σ définie sur l'ensemble de battements $\mathbb{B}$ qui est un sous espace de $L^2(\mathbb{R})$

$$\sigma : \mathbb{B} \times \mathbb{B} \to [0,1], \qquad \sigma(\Psi, \Psi') = \frac{\langle \Psi | \Psi' \rangle}{\|\Psi\| \cdot \|\Psi'\|} \tag{7}$$

Chaque enregistrement ECG est un ensemble de battements S. Cet ensemble est partitionné en k clusters, $(k \leq n)$, $S = S_1 \cup S_2 \ \cup \cdots \cup \ S_k$. Chaque cluster S_i, $0 \leq i \leq k$ est défini par:

$$S_i = \{x \in S - \bigcup_{j<i} S_j : r \leq \sigma(c_i, x) \leq 1\}$$

où c_i (centroide de S_i) est un battement pris aléatoirement dans $S - \bigcup_{j<i} S_j$, σ la fonction de similarité donnée précédemment et r le degré minimal de similarité.

Le classificateur utilise en plus de la fonction de similarité la régle suivante pour ajuster le type d'un battement. Si la classe du battement trouvée avec la fonction de similarité est N, LBBB ou RBBB, le ration RR_{av}/RR_{ap} est calculé. Si $RR_{av}/RR_{ap} < (1 - \epsilon_1)$ ou $(RR_{av} + RR_{ap}) < (2RR_m - \epsilon_2)$ alors la classe est changée en APB sinon elle reste inchangée.

0.2.4 Localisation

Les signaux ECG du MIT-BIH arrhythmia database sont des enregistrements de 30 minutes (parfois un peu plus) échantillonées à 360 points par seconde ce qui leur donne une longueur d'au minimum de $N = 648000$ points. Avec l'analyse multirésolution, la plus grande résolution des ces signaux est $J = 19$. Nous définissons le sous ensemble $\prod_\theta = \{k \in \mathbb{Z} : |c_{J-1,k}| > \theta, \ \theta \in \mathbb{R}\}$ des coefficients d'ondelettes obtenus à la première décomposition du signal ECG. Cet ensemble est appelé **set of parsimony** parce qu'il constitut la seule information que nous utilisons pour analyser le signal.

Un masque est défini pour reconnaitre les complexes QRS et ainsi localiser le battement. Pour tout $k \in \prod_\theta$, nous appliquons le masque $M_{nqrs} : \prod_\theta \to \{0, 1\}$. Si $M_{nqrs}(k) = 1$ alors le segment du signal ECG autour du point correspondant à l'intant $k/2^{J-1}$ est un potentiel complexe QRS.

Le fonctionnement du masque M_{nqrs} est décrit par l'algorithme suivant lorsque la décomposition en ondelette est faite avec l'ondelette de Haar.

La justification de l'utilisation de ce masque peut être résumée comme suit. A la première décomposition du signal ECG avec l'ondelette de Haar, les seuls coefficients d'ondelettes dont la valeur absolue est supérieure à un certains seuil sont ceux dont le support est confondu avec celui d'un complexe QRS. En plus le complexe QRS commence par une pente négative prononcée suivi d'une pente positive (voir figure 3) donc si nous trouvons un maximun local c_{J-1,k_1} précédé d'un minimum local c_{J-1,k_0} et que $k_1 - k_0$ est assez petit nous avons un complexe QRS.

Require: integer $k \in \mathbb{Z}$;
integer $w > 0$;
set $A = \prod_\theta \cap [k-w, k+w]$;
sequence $(c_{J-1,l})_{l \in \{k-w,\ldots,k+w\}}$;
real parameters θ_0 and θ_1 with $0 < \theta_1 \leq \theta_0$.
Ensure: M_{nqrs}.
for $m \in A$ **do**
  $M_{nqrs}(m) \leftarrow 0$
  $k_0 \leftarrow \arg\max\{c_{J-1,l} : l \in A, |l-k| \leq w\}$
  $k_1 \leftarrow \arg\min\{c_{J-1,l} : l \in A, l - k_0 > -w\}$
  if $c_{J-1,k_0} > \theta_0 \quad \& \quad c_{J-1,k_1} < -\theta_1$ **then**
    $M_{nqrs}(k_0) \leftarrow 1$
  end
end

0.3 Application et résultats obtenus

Nous avons tester nos méthodes de classification et de localisation sur le MIT-BIH arrhythmia database. C'est une base de données contenant 48 enregistrements (de 30 minutes chacun) d'électrocardiogrammes. Ces enregistrements sont obtenus à partir de 47 sujets étudiés par le BIH Arrhythmia Laboratory entre 1975 et 1979. Ils sont échantillonés à 360 points par seconde et annotés séparément par deux ou plusieurs cardiologues.

La performance du classificateur a été évaluée en termes de taux d'exactitude dans la reconnaissance des arythmies par signal ECG et par taux d'exactitude par classe de battements cardiaques. Les résultats obtenus sont résumés dans les tableaux 1,2,3.

0.4 Conclusion

Cette thèse a porté sur l'analyse des électrocardiogrammes en vu de développer de nouvelles méthodes efficaces de classification des arythmies (un outil de diagnostique) et de localisation et détection automatique des battements normaux en temps réel dans un signal ECG (un outil de surveillance).

Les signaux ECG sont traités, les battements extraits compressés et analysés à l'aide d'ondellettes. La méthode de classification proposée exploite les spécificités du patient en faisant un regroupement contextuel des battements et en utilisant une base de données de battements cardiaques annotés. La méthode utilise également une fonction de similarité

Table 1: Résultat de classification par enregistrement.

Numéro enregistrement	Nombre de battements	Nombre de battements mal classés	Taux de réussite (%)
100	1892	0	100
101	1514	2	99.87
103	1721	5	99.71
105	2141	71	96.68
106	1688	52	96.92
107	1776	11	99.38
108	1468	53	96.39
109	2089	11	99.47
111	1768	41	97.68
112	2101	2	99.90
113	1498	3	99.80
114	1590	44	97.23
115	1628	1	99.94
116	2007	23	98.85
117	1277	3	99.77
118	1907	42	97.80
119	1653	0	100
121	1551	5	99.68
122	2044	0	100
123	1262	0	100
124	1334	12	99.10
200	2156	76	96.47
201	1408	44	96.88
202	1860	63	96.61
203	2467	592	76
205	2180	6	99.72
207	1475	21	98.58
208	2122	19	99.10
209	2509	109	95.66
210	2164	57	97.37
212	2275	7	99.69
213	2450	40	98.35
214	1866	86	95.39
215	2780	104	96.26
217	1608	12	99.25
219	1764	44	97.51
220	1685	36	97.86
221	2011	2	99.90
222	1892	279	85.25
223	2166	265	87.77
228	1695	29	98.29
230	1849	2	99.89
231	1270	12	99.06
232	1478	16	98.92
233	2543	44	98.27
234	2231	0	100
Average			97.52

Table 2: Résultat de classification par classe de battements.

Classe de battements	Nombre de battements	Nombre de battements mal classés	Taux de réussite (%)
NB	61896	638	98.96
PB	2952	6	99.80
LBBB	6856	49	99.29
RBBB	5870	44	99.25
APB	2270	414	81.76
PVC	5969	1195	79.97

Table 3: Comparaison avec d'autres méthodes de classification.

Méthode	Nombre de classe de battements	Taux de réussite (%)
ICA [15]	6	99.51
FTNN [8]	3	98
MOE [12]	4	94
MRANN [9]	13	96.79
FHNN [1]	7	96.6
Méthode proposée	6	97.52

pour comparer deux battements donnés.

La méthode de localisation exploite aussi la décomposition en ondelette mais se base sur une partie des données disponibles (**set of parsimony**) pour détecter automatiquement et temps réel à l'aide d'un masque les battements cardiaques normaux contenus dans le signal ECG.

Les deux méthodes ont été testées sur les signaux électrocardiogrammes du MIT-BIH arrhythmia database et de bon résultats ont été obtenus. Cependant pour la classification il serait intéressant de pourvoir réduire le volume de données à annoté et à inclure dans la base de données des battements. Une solution pour contourner cette difficulté serait de diminuer la redondance de ces données. Pour la localisation, l'avis d'un expert cardiologue sur la fonction masque utilisée est nécessaire. Aussi la localisation des ondes P et T pourrait améliorer la détection des battements anormaux.

Table 4: Résultat de la localisation par enregistrement.

File identifier	Our normal	MIT marked	MIT normal	Coincidences	False positive	False negative
100	2274	2237	2203	2202	34	0
101	1853	1840	1826	1812	6	13
102	1694	2156	99	0	9	98
103	2256	2057	2048	2047	169	0
104	2281	2272	163	101	2005	61
105	730	2650	2487	652	75	1822
106	1741	2063	1473	1405	298	67
107	462	2104	0	0	0	0
108	70	1791	1710	63	5	1455
109	1133	2488	0	0	0	0
111	3	2098	0	0	0	0
112	177	2507	2494	175	1	2215
113	1795	1767	1761	1760	5	0
114	913	1863	1793	873	34	919
115	1953	1931	1922	1921	0	0
116	2395	2382	2263	2242	112	20
117	1434	1514	1509	1392	16	116
118	2332	2264	0	0	0	0
119	1544	2061	1519	1518	0	0
121	0	1846	1831	0	0	0
122	2474	2434	2431	2428	0	2
123	1515	1495	1491	1490	0	0
124	1804	1609	0	0	0	0
200	1552	2747	1715	1337	184	373
201	535	1995	1581	496	17	1082
202	1638	2120	2036	1593	36	442
203	1449	3055	2482	1136	254	1325
205	2541	2628	2527	2482	14	44
207	41	2356	0	0	0	0
208	1953	2986	1561	1540	380	20
209	3048	3006	2575	2573	428	1
210	1458	2639	2381	1423	29	957
212	2788	2718	923	922	1770	0
213	3126	3239	2586	2584	486	1
214	2142	2298	0	0	0	0
215	3378	3344	3144	3128	194	15
217	1079	2244	244	243	501	0
219	2122	2276	2046	2042	43	3
220	2048	2033	1918	1917	94	0
221	2013	2424	1999	1964	16	34
222	1601	2596	2024	1292	293	731
223	2023	2603	1990	1817	165	172
228	312	2100	1659	22	280	1629
230	2263	2422	2214	2213	8	0
231	1565	1979	314	313	1105	0
232	1312	1787	0	0	0	0
233	2577	3099	2195	2164	365	30
234	2740	2718	2654	2642	51	11

Chapter 1

Introduction

An electrocardiogram, also called ECG, is a recording of the electrical activity of the heart. This electrical activity is responsible for contractions that expel and aspirate blood from the heart thus generating blood flow throughout the body. Recorded from electrodes placed on the surface of the skin at the breast, this electrical activity heart can be represented graphically, and allows doctors to determine whether the functioning of the heart is normal or not. The electrocardiogram has become one of the most important tools in the diagnosis of heart diseases. From the ECG of a patient, a cardiologist can analyze the shape of the heartbeat and diagnose the disease from which he suffers. It is also used as a searching tool for potential heart rhythm disorders that may result from the of use new drugs. Abnormalities of the heart may be rare and scattered in a long electrocardiogram tracing, therefore the work of cardiologists consisting in tracking down these irregularities can be tedious. It becomes necessary to develop software diagnostic aid. The population of older people living alone is increasing more and more, thus developing monitoring tools that detect in real-time irregularities of the heart and alert the nearest medical center has become an urgent matter.

Over the past few years implementing automatic systems has gained more and more interest in the field of ECG diagnosis. The ECG signal is first preconditioned ie, filtered to eliminate different types of noise, segmented, delineated with respect to their waves and complexes, etc. But the great difficulty in implementing these software solutions lies in the wide variety in the shape of heart beats belonging to a given class of arrhythmia and the similarity in the shape of beats belonging to different classes. Therefore, algorithms for computer-based diagnosis generally have three steps: ECG beat detection (localization), extraction of useful features from beats, and analysis.

Some methods have been developped for ECG beat localization, but none of them

proves universally acceptable accuracy. Therefore efforts are constantly deployed for their enhancement. The main difficulty in automatic heart beat detection is due to the noise corrupting the electrocardiogram, and sometimes the signal to noise ratio can be very low. These methods are based on: amplitude emphasizing, digital filtering, heuristic decison rules, etc.

Feature (useful information) extraction can be done in the time domain, in the frequency domain, by multiscale decomposition, by multifractal analysis, or by statistical means.

Various classification methods are developped and can be grouped into two groups:

- **unsupervised methods** using Linear Discriminant Analysis, Learning Vector Quantization, various clustering techniques, etc.
- **supervised methods** using domain knowledge, exhaustive search, heuristic decison rules, etc.

Same remarks as for localization applies here: most of the methods does not proves universally acceptable accuracy in regard to the facts exposed by the the American Heart Association Electrocardiography and Arrhythmias Committee in the paper "Recommendations for the standardization and interpretation of the electrocardiogram" that the percentage of ECGs correctly classified by the computer programs have a median of 91.3%. In addition, it appears that those which shows good results are not usually tested on a large database (for example the Independent Component Analysis method proposed by S. Yu and K. Chou).

1.1 Objectives of this Thesis

The main objective of this thesis is to develop an efficient and accurate method of ECG beat classification. The latter must be able to classify six types of heart beat, namely normal beats (NBs), premature ventricular contractions (PVCs), paced beats (PBs), atrial premature beats (APBs), left bundle branch block beats (LBBBs), and right bundle branch block beats (RBBBs). The second main point is to localise in real time ECG QRS complexes that indicate normal heart beats (thus localizing abnormal ones). Theses objectives are achieved by following some steps:

1. **ECG signal noise reduction:** ECG recordings are generally corrupted by noise from various sources. Then techniques of low-frequency and high-frequency noise cancellation based on wavelet transformation (which is a powerful tool for non-stationary signal analysis) have been used.

2. **Morphological Feature Extraction:** Significant information from ECG signals are extracted. Also the power of wavelet approximation have been used to dimmensionnaly reduce the amount of information to analyse.

3. **Exploitation of (patient) specificities:** The classification method developped in this thesis is patient-adaptable. A database of patient annotated heart beats have been build. A clustering method has also been used to emphasize patient specificities carried by the ECG signal.

4. **Analysis:** After extracting morphological features and exploiting patient spécificities, analysis to classify and to localise heart beats has been done.

1.2 Organization of the Thesis

The thesis is organized in six chapters. After the introductory one, chapter 2 provides usefull medical and technical informations for the understanding of ECG signals. It also describes morphologies of normal heart beats and of different arrhythmias.

Chapter 3 gives wavelet multiresolution analysis background and describes the cascade algorithm for computing discrete wavelet transform.

In chapter 4, we present our method of heart beat classification based on wavelet transform. The method uses waveform similarity and RR intervals as important features for the classification of six types of heart beat, namely normal beats, atrial premature beats, paced beats, premature ventricular contractions, left bundle branch block beats, and right bundle branch block beats.

Chapter 5 addresses our parsimonious and computationally efficient method of QRS complexe localization. It automatically analyse electrocardiograms with the help of wavelet bases, localise points of interest and decide whether they are normal or not.

Chapter 6 concludes this thesis. It describes results obtained with our methods and future improvement possibilities.

Chapter 2

Electrocardiograms (ECG)

In this chapter we provides usefull medical and general informations for the understanding of ECG signals. A description of the morphologies of normal heart beats and of different arrhythmias is done. We finish this chapter with a description of the MIT-BIH arrhythmia database which we have used in order to test our methods.

Description of arrhythmias are mainly from [22, 24, 25, 30, 32, 23].

2.1 What is an Electrocardiograms ?

With the invention of the string galvanometer by the Dutch physiologist, W. Einthoven, the electrocardiogram has become a valuable tool of studying the electrical activity of the heart. The heart is the muscular organ located in the chest between the lungs which, with regular rhythmic contractions cause blood to circulate throughout the body (see figure 2.1 for an anatomy).

The electrocardiogram, also called ECG signal is a biological signal which is recorded from electrodes placed on the body surface. It represents the electrical activity of the heart, which is at the origin of the cardiac muscle contraction that results to the propel of the blood from vena cavas to aorta and pulmonary artery.

Clinicaly the electrical activity of the heart is represented by various signals called, the 12-lead ECG system. The 12-lead ECG system uses 10 electrodes placed at various positions on the body. Three of them are from the Einthoven lead system illustrated in figure 2.2. The Einthoven lead system can be discribes by the equilateral triangle formed by the position of the three electrodes, one on the right arm (RA), one on the left arm

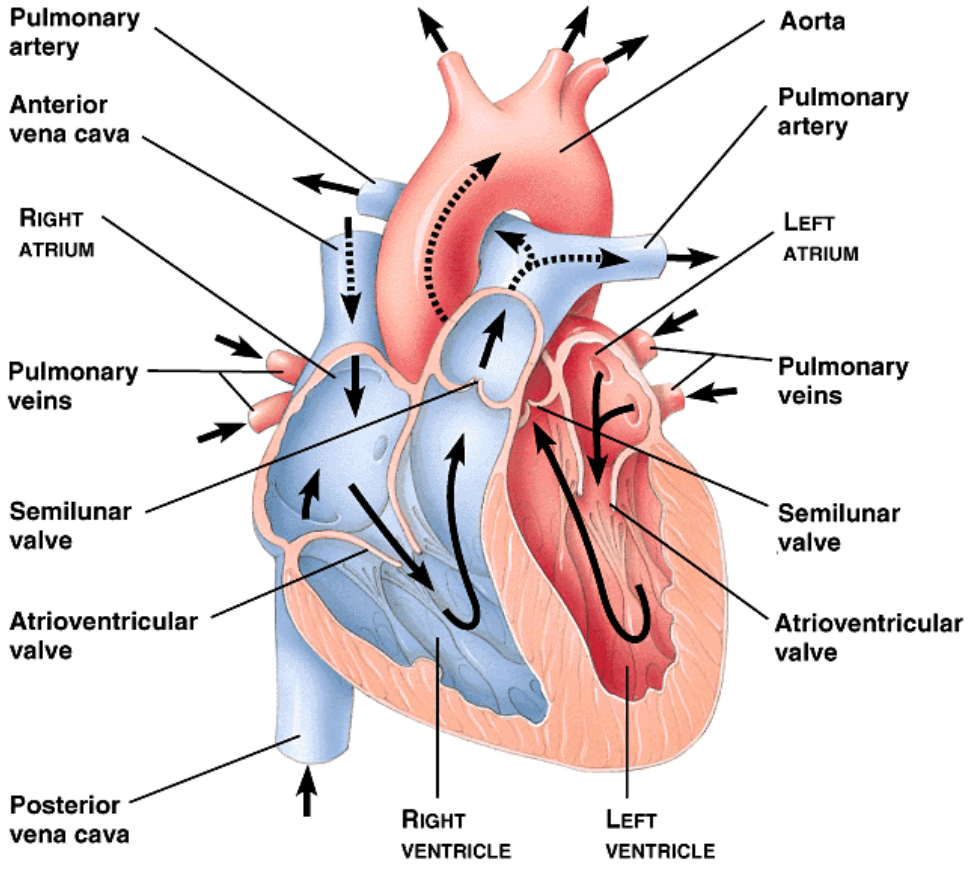

Figure 2.1: The heart Structure. Figure is adapted from [29]

(LA) and another on the left leg (LL). It gives the voltage between RA, LA and LL points as follow:

$$\begin{aligned} I &= \phi_{LA} - \phi_{RA} \\ II &= \phi_{LL} - \phi_{RA} \\ III &= \phi_{LL} - \phi_{LA}, \end{aligned} \tag{2.1}$$

where ϕ_{LA} is the potential at the left arm, ϕ_{RA} the potential at the right arm and ϕ_{LL} the potential at the left leg.

Within the 12 leads three other are from the use of the Wilson Central Terminal (WCT) introduced by Frank Norman Wilson (Wilson et al., 1934). The Wilson central terminal is a point from which are connected by wire a 5 $k\Omega$ resistance to each of the three electrodes of the Einthoven triangle (Figure 2.3)

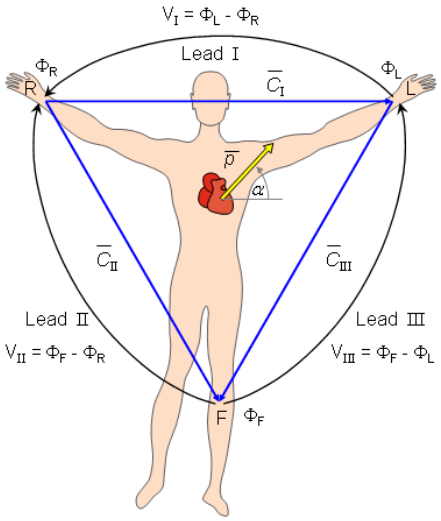

Figure 2.2: Einthoven lead system and Einthoven triangle. Figure is adapted from [4]

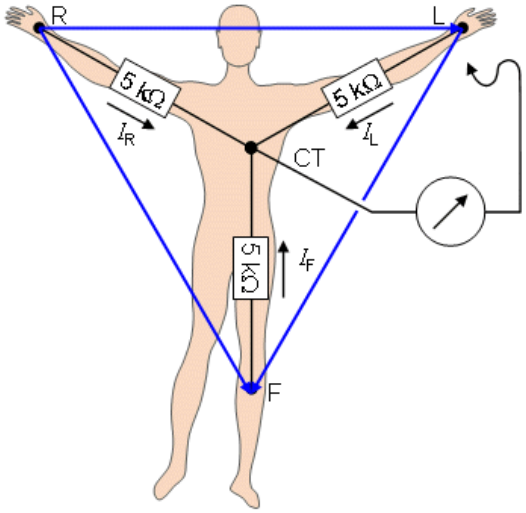

Figure 2.3: The circuit of the Wilson central terminal (WCT) using the Einthoven triangle. Figure is adapted from [4]

The three leads obtained from the WCT are V_{LA}, V_{RA} and V_{LL} and represent the potential between each electrode of the Einthoven triangle and the Wilson central terminal. The shortcoming of these leads is there signals are weak. Therefore E. Goldberger find that they can be augmented by removing the resistance from the Wilson central terminal

(Figure 2.4). The improvement of the leads V_{LA}, V_{RA} and V_{LL} by E. Goldberger gives the augmented leads (aV_{LA}, aV_{RA} and aV_{LL}) because of the augmentation of the signal.

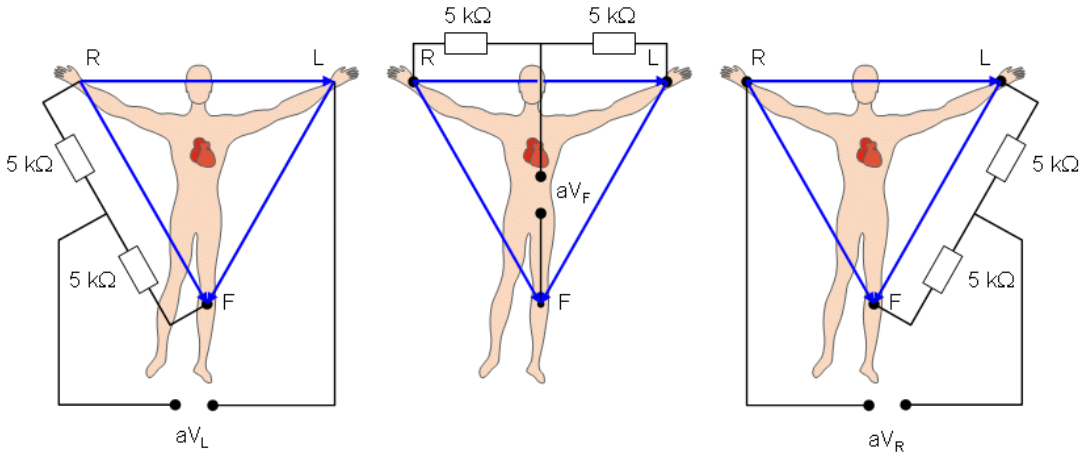

Figure 2.4: The circuit of the Goldberger augmented leads. Figure is adapted from [4]

The 6 remaining leads from the 12 are also introduced by F. N. Wilson for measuring the potentials close to the heart, they are called precordial leads and are denoted by V_1, V_2 to V_6. These leads are positionned on the chest as shown on Figure 2.5.

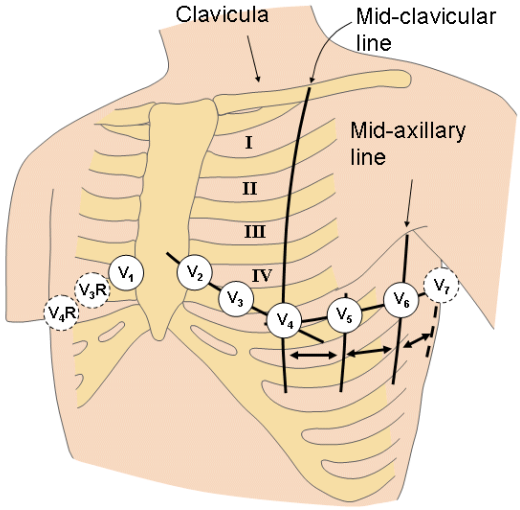

Figure 2.5: The Wilson precordial leads. Figure is adapted from [4]

Finally the 12-lead ECG system is a set of 12 signals denoted as:

- The Einthoven lead system: I, II, III;
- the augmented leads: aV_{LA}, aV_{RA}, aV_{LL};
- the precordial leads: V_1, V_2, V_3, V_4, V_5, V_6.

The ECG signals are generaly distorted due to artifact from muscular activity, respiration, and poor electrode contact. In order to reduce the signal distorsion R. E. Mason and I. Likar recommend placement of the electrodes on parts of the body which cause less noise. The electrodes are then moved from the arms and leg in the standard 12-lead system to the shoulders and the hip (see Figure 2.6). These modifications in the standard 12-lead system are very important and are known are Mason and Likar lead system.

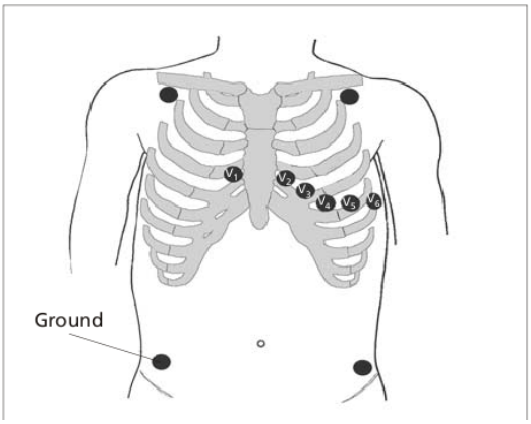

Figure 2.6: The Mason-Likar 12-lead system. Figure is adapted from [5]

Figure 2.7 and 2.8 illustrates an ECG 12-lead system captured from a 26-year-old healthy person. The start point of each lead is shown by a verticle thick segment at the side of the lead's name.

2.2 Characteristics of the normal ECG

The waveform of signals in the ECG 12-lead varies from person to person depending on age, body size, gender, and many other variables. Therefore the normal ECG can be in a wide range. Nevertheless, there are significant characteristics shared by normal ECGs. Figure 2.9 shows components of a normal ECG cycle (heart beat).

As we can see it in the Figure 2.9 un normal ECG beat is composed of some elements which are P wave, PR interval, QRS complex, ST segment, QT interval and T wave.

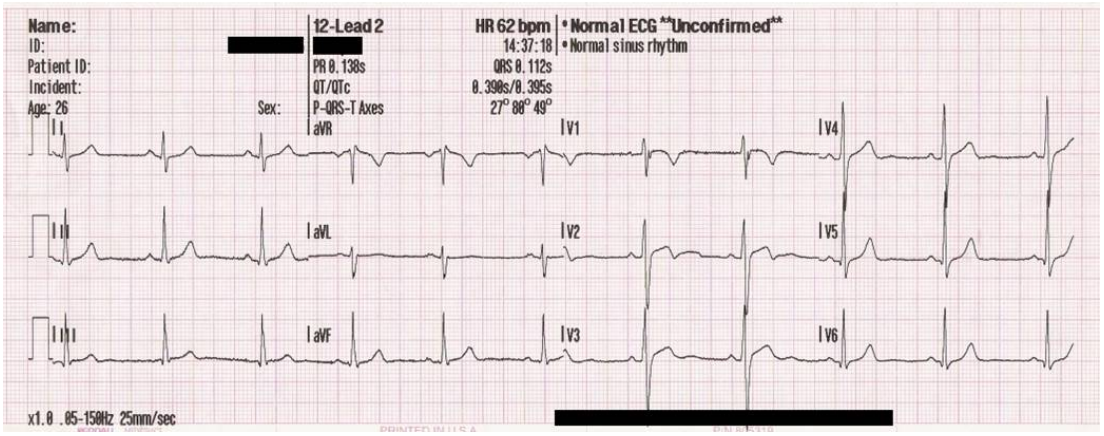

Figure 2.7: The ECG 12-Lead of a 26-year-old male. Figure is adapted from [19]

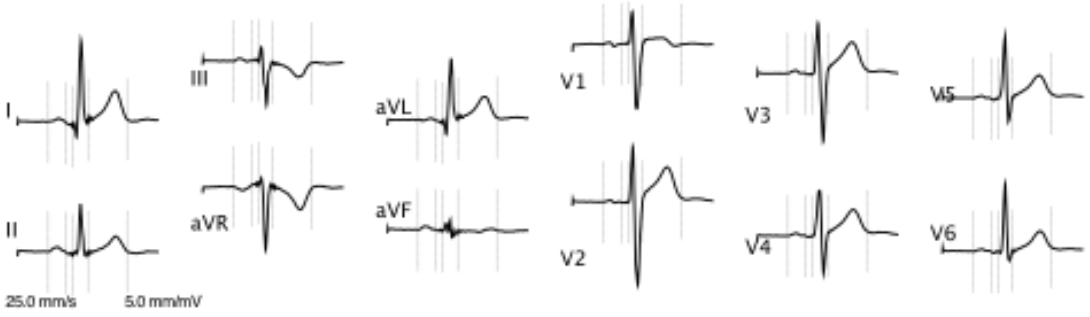

Figure 2.8: A cycle (heart beat) of each lead in the ECG 12-Lead system [20]

2.2.1 The P wave

The P wave represents the sequential activation of the right and left atria. Its normal duration is between 0.08 and 0.12s. Its amplitude must be less than 2.5 mV [22]. The shape of the P wave is smooth and entirely positive.

2.2.2 The PR interval

The PR interval is the portion on the ECG beat beginning at the start of the P wave to the start of the QRS complex. Its normal duration is from 0.12 to 0.20s The PR interval is composed of the P wave and the PR segment which is a segment with no wave or deflection (isoelectric). Although the PR segment is flat, the atrials are actually contracting, filling

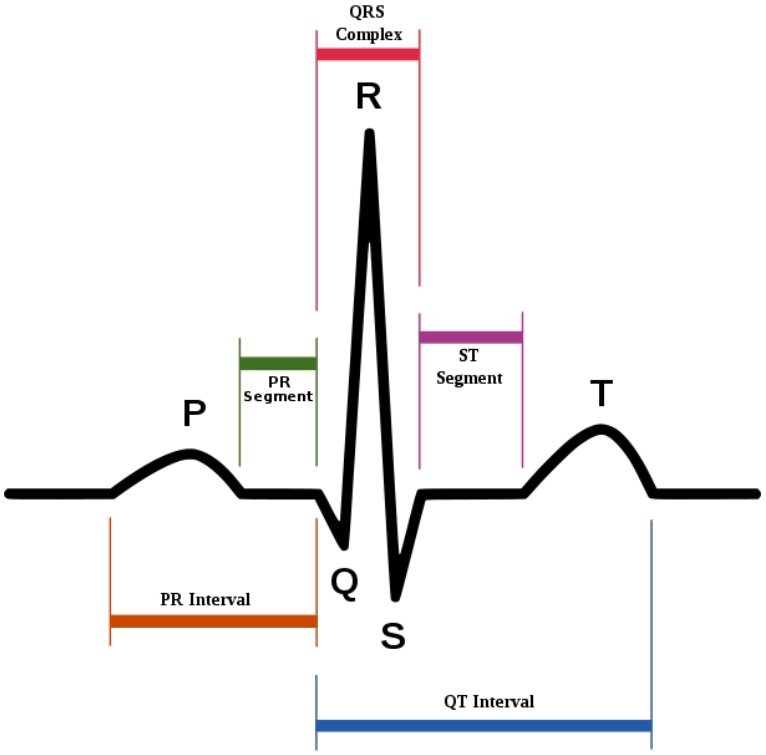

Figure 2.9: Schematic representation of normal ECG cycle. Figure is adapted from [21]

the ventricles before ventricular systole.

2.2.3 The QRS complex

The QRS complex represents the simultaneous activation of the right and left ventricles. The normal QRS duration range is from 0.06 to 0.10s [22]. Ventricles are the more muscle mass part of the heart, therefore the amplitude of the QRS complex is considerably higher than other waves of heart beat.

2.2.4 The ST segment

The ST segment represents the period from the end of ventricular depolarization to the beginning of ventricular repolarization. The ST segment is a short isoelectric line between the end of the QRS complex and the initial deflection of the T wave.

2.2.5 The QT interval

The QT interval starts from the beginning of the QRS complex to the end of the T wave. It indicates the duration of ventricular depolarization and repolarization. The QT interval as well as the corrected QT interval (QT_c) are important in the diagnosis of long QT syndrome and short QT syndrome. The QT interval depends on the heart rate, and various correction factors have been developed to correct the QT interval for the heart rate. The most commonly used method for correcting the QT interval for heart rate is the one formulated by Bazett:

$$QT_c = \frac{QT}{\sqrt{RR}}, \tag{2.2}$$

where RR is the interval from R peak of one QRS complex to R peak of the next QRS complex, measured in seconds. An another formula for correcting th QT interval is the "Poor Man's Guide" to upper limits of QT. For $HR = 70bpm$, $QT < 0.40sec$; for every $10bpm$ increase above 70 subtract 0.02 sec, and for every $10bpm$ decrease below 70 add 0.02 sec. For exemple if $HR = 80bpm$ then $QT < 0.38$ and if $HR = 60bpm$ then $QT < 0.42$. HR is the Heart Rate and bpm means beats per minute.

2.2.6 The T wave

The T wave represents the ventricular repolarization and is the first deflection following the QRS complex. The T wave can de sometimes followed by a small wave similar to the P wave called U wave.

2.2.7 Morphology of the normal ECG

It is important to remember that there is a wide range of normal variability in the 12 lead ECG. Therefore the morphology of the normal ECG can be slightly different see figure 2.2.7.

2.3 ECG abnormalities

The abnormamlities in an ECG are generaly linked to cardiopathy or heart disease. They can also be linked to disorders of the regular rhythmic beating of the heart called arrhythmias. We recall that cardiopathy is one of the leading cause of death in the world [24, 25]. The cardiopathy can be various but in this thesis we will focus on the five we are about to identify automatically in an ECG.

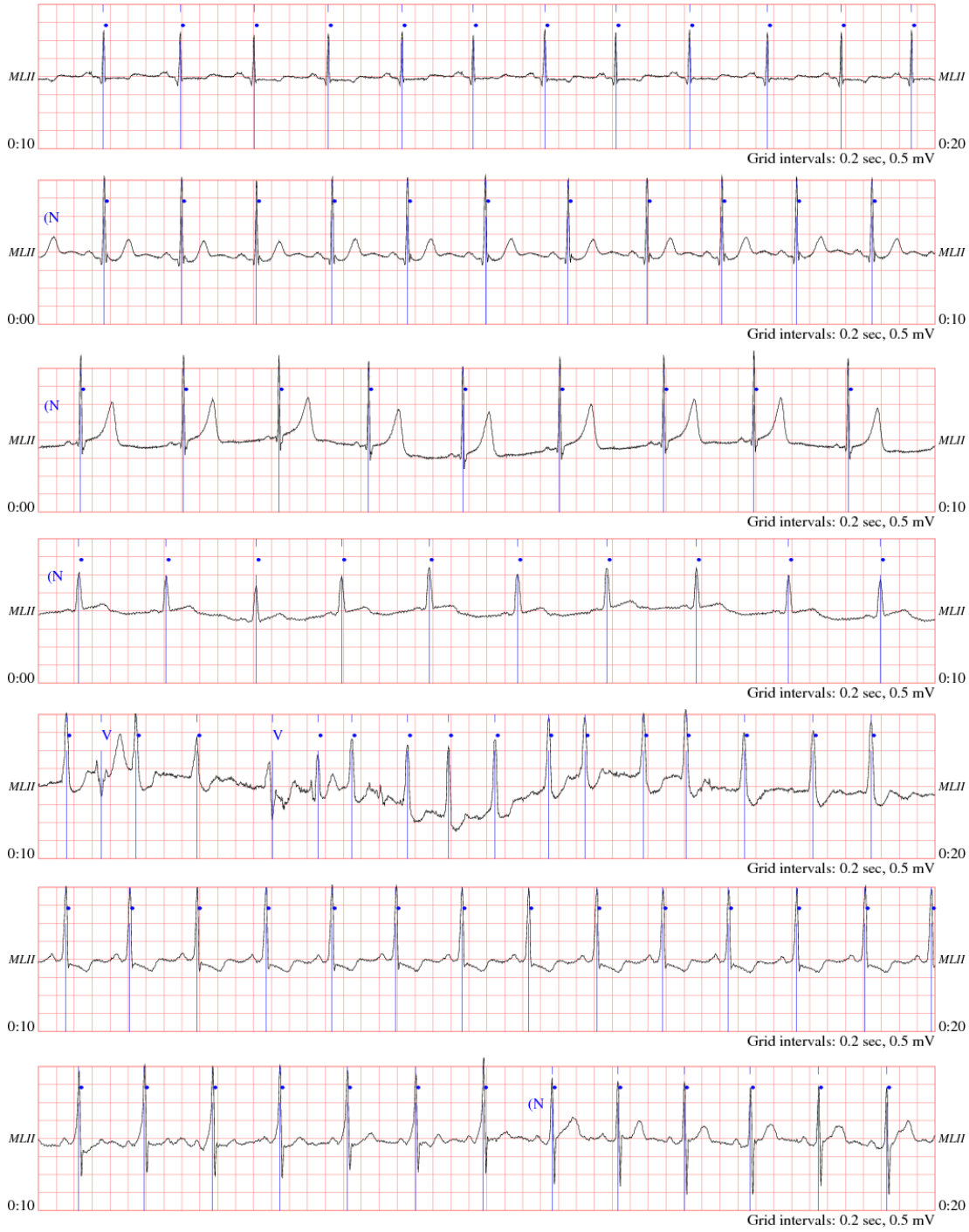

Figure 2.10: Differents morphologies of the normal heart beats. Normal Beats are marked •. Segments of ECGs are taken respectively from records: 100, 103, 113, 121, 203, 223, 230 of the MIT-Arrhythmia Database [23]

Right Bundle Branch Block (RBBB)

The right bundle branch block occurs when the right ventricle is depolarized after the left ventricle. This happens when the transmission of the electrical impulse is delayed or not conducted along the right bundle branch, however, the left ventricle is normally activated by the left bundle branch. In normal beats the QRS complex is narrow (< 0.1s) because the two ventricles (left and right) receive the electrical impulse at the same time. While in the RBBB the right ventricle receives the electrical impulse after the left ventricle. Therefore the QRS complex is widen. In the "incomplete" RBBB has a QRS duration of 0.10 to 0.12s, the QRS complex of the "Complete" RBBB can be greater than 0.12s [22]. See figure 2.3.

Left Bundle Branch Block (LBBB)

The left Left bundle branch block is the opposite of Light bundle branch block. Here the left ventricle is depolarized after the right ventricle. But LBBB is usually associated with increased rate of mortality than RBBB. While RBBB often occurs in young patient without apparent organic heart disease, LBBB is more often encountered in older patients and indicates underlying cardiac pathology such as dilated cardiomyopathy, hypertrophic cardiomyopathy, hypertension, aortic valve disease, coronary artery disease. [26]. See figure 2.3.

Atrial Premature Beat (APB)

The atrial premature beat is a kind of disturbance in the normal heartbeat that manifests as an early beat originating in the atria. Atrial premature beats (APB) can occur in persons with normal or diseased hearts. Therefore they are not associated with heart disease. In up to 64% of healthy young individuals, some APBs are found in an ambulatory electrocardiogram, and in most cases without symptoms [27]. APBs may be associated with stress, fatigue, alcohol, smoking heart failure, pulmonary congestion, and pulmonary hypertension. Physical examination can reveal APBs but must be confirmed by electrocardiograms. Schematically the atrial premature beat has a deformed p wave, it may be obvious or be buried in the T wave of the preceding beat. Depending on the origin of the impulse in the atria (high atria or low atria) P waves can be positive or negative in leads II, III and aVF. The QRS complex of an APB has often a normal duration but sometimes is prolonged [28]. APBs can occur as single or repetitive events. The pause after an APB is usually incomplete; i.e., the interval from sinus to atrial premature beat plus the next sinus beat measures less than two sinus cycles (see Figure 2.15) [22]. See figure 2.3.

Premature Ventricular Beat (PVC)

Premature ventricular contractions are heart beats originating from the ventricles rather than from the sinoatrial node which is the initiator of the normal beats. Premature ventricular contractions are premature beats because they occur before the regular heart beat. Morphologically PVCs are characterized by QRS complexes usually wider than 0.12s. These complexes are not preceded by a P wave, and the T wave is usually large, and its direction is opposite the major deflection of the QRS. PVCs can occur as single or repetitive events. Usually a PVC is followed by a complete compensatory pause; i.e., the interval from sinus to premature ventricular beat plus the next sinus beat measures two sinus cycles (see Figure 2.15) [22]. PVCs are usually not associated with any increased rate of mortality, but the presence of high PVC frequencies ($>$ 20 per hour or $>$ 10 per thousand beats) can lead to sudden coronary death[30]. See figure 2.3.

Paced Beat (PB)

Paced beats, PVCs, and beats arising in the presence of bundle branch block (BBB) share similar ventricular activation sequence and are accepted to closely resemble each other. The paced beat has also a wide QRS complex because the complex does not use a normal conduction system and depolarizes the ventricular from right to left[31]. Paced beats can unmask new or old myocardial infarction when sinus beats fail to exhibit the typical infarct pattern [32]. See Figure 2.3.

2.4 The MIT-BIH arrhythmia database

In this thesis we have used the MIT-BIH Arrhythmia Database which is an annotated ECG Databases. The MIT-BIH Arrhythmia Database is a product of the Beth Israel Deaconess Medical Center distributed in 1980. It contains 48 half hour excerpts of two channel ambulatory ECG recordings (the modified limb lead II and one of the leads V1, V2, V4 or V5), obtained from 47 subjects studied by the BIH Arrhythmia Laboratory between 1975 and 1979. The recordings were digitized at 360 samples per second per channel with 11-bit resolution over a 10 mV range. Two or more cardiologists independently annotated each record; disagreements were resolved to obtain the computer-readable reference annotations for each beat (approximately 110,000 annotations in all) included with the database [23]. The MIT-BIH Arrhythmia Database is used in many works in the field of ECG signal processing and classification.

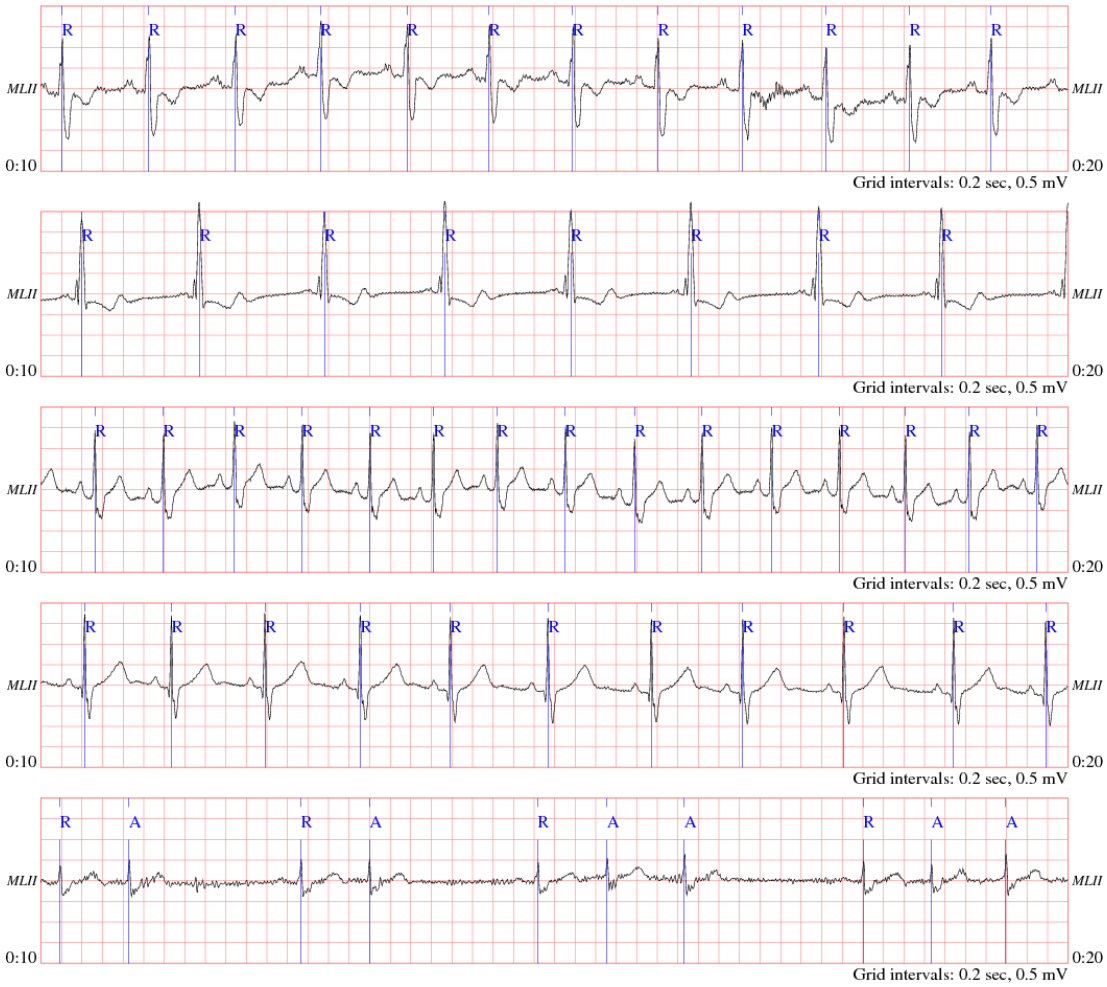

Figure 2.11: Differents morphologies of heart beats of RBBB class. RBBB are marked R. Segments of ECGs are taken respectively from records: 118, 124, 212, 231, 232 of the MIT-Arrhythmia Database [23]

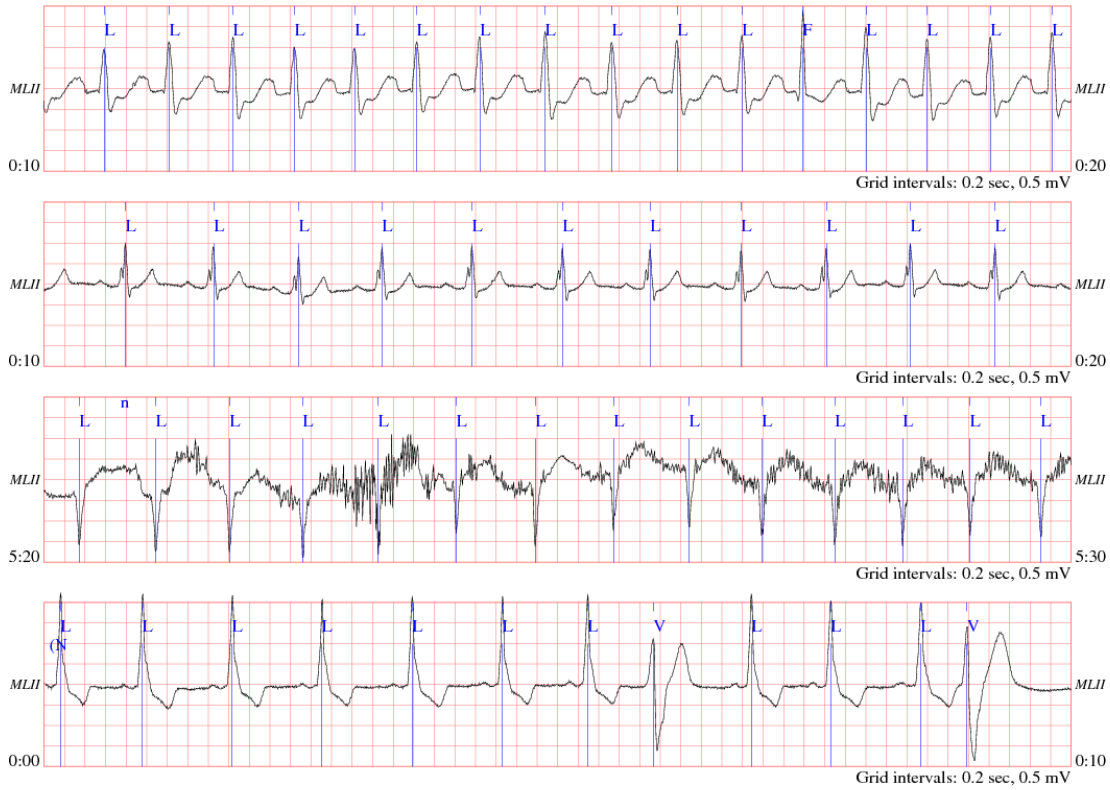

Figure 2.12: Differents morphologies of heart beats of LBBB class. LBBB are marked ʟ. Segments of ECGs are taken respectively from records: 109, 111, 207, 214 of the MIT-Arrhythmia Database [23]

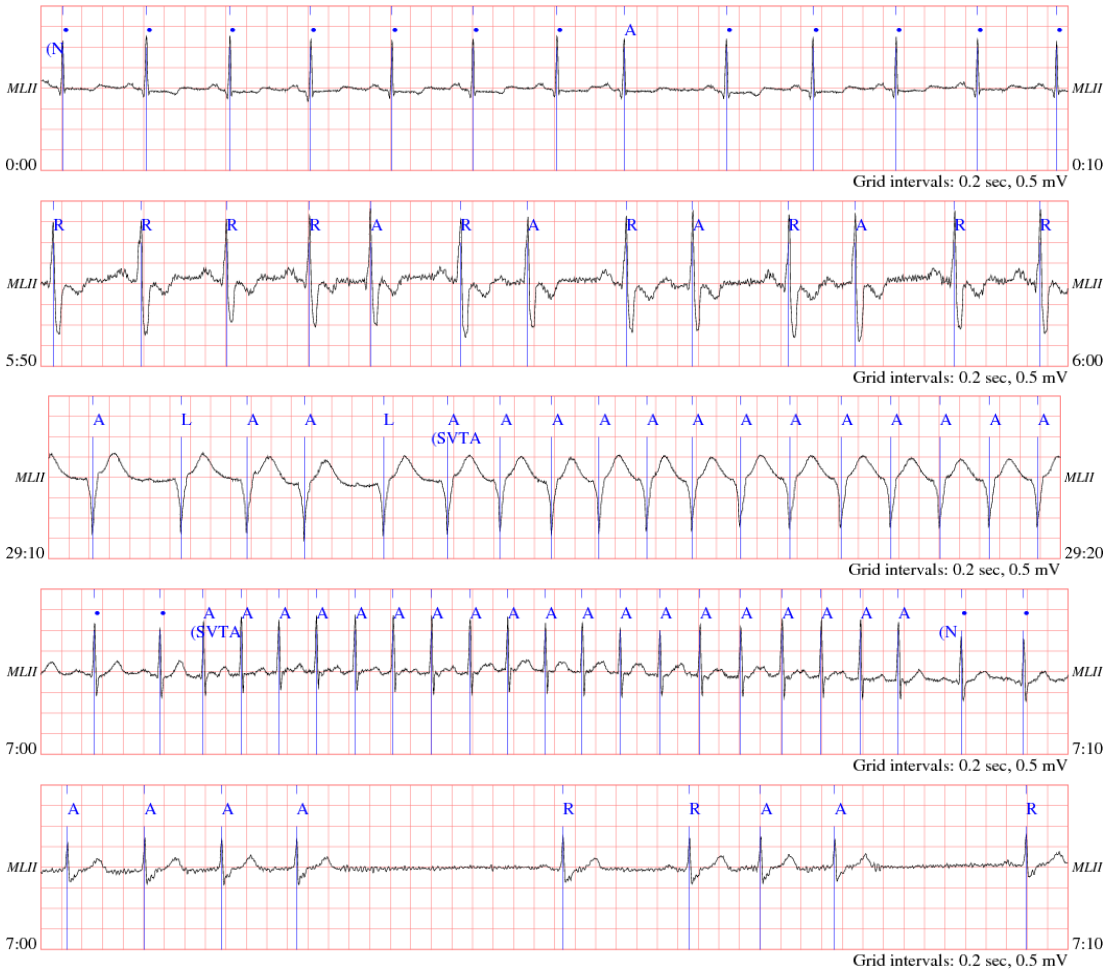

Figure 2.13: Differents morphologies of heart beats of APB class. APB are marked $^{\text{A}}$. Segments of ECGs are taken respectively from records: 100, 118, 207, 209, 232 of the MIT-Arrhythmia Database [23]

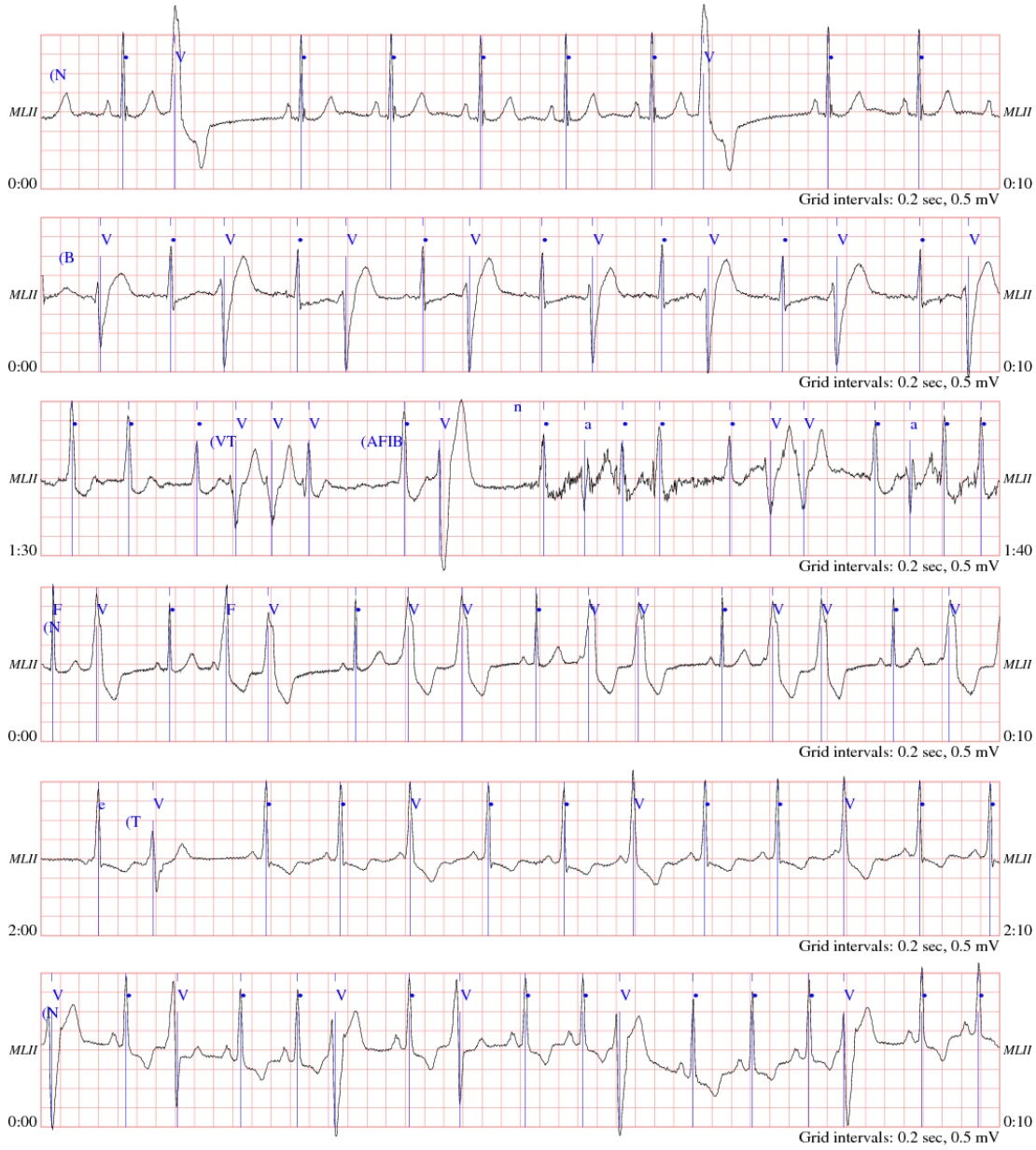

Figure 2.14: Differents morphologies of heart beats of PVC class. PVC beats are marked V. Segments of ECGs are taken respectively from records: 119, 200, 203, 208, 223, 233 of the MIT-Arrhythmia Database [23]

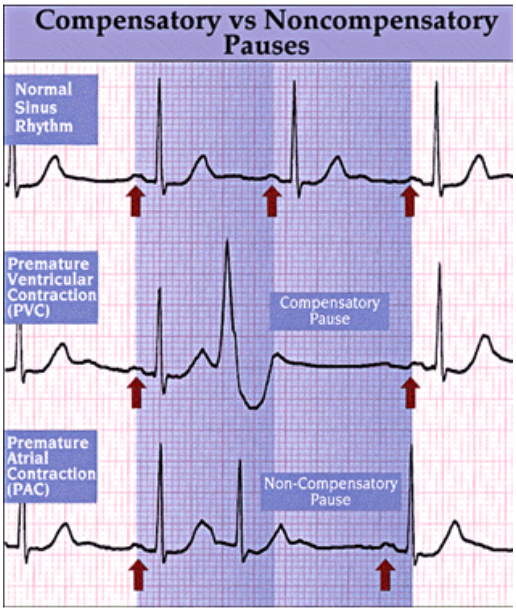

Figure 2.15: Compensatory and Noncompensatory pause. Figure is adapted from [22]

Figure 2.16: Differents morphologies of heart beats of Paced class. Paced beats are marked /. Segments of ECGs are taken respectively from records: 107, 217 of the MIT-Arrhythmia Database [23]

Chapter 3

Wavelets

There are different ways to introduce wavelets. According to [38], we define wavelets as denumerable families of functions on $\mathbb{R}$ satisfying the following properties:

1. they form a basis of $L^2(\mathbb{R})$ with suitable orthogonality properties to be defined later,
2. they are indexed by integer translations, i.e. mappings $t \mapsto t + k$, with $k \in \mathbb{Z}$ for all $t \in \mathbb{R}$, and integer powers (often dyadic) of scaling, i.e. mappings $t \mapsto 2^j t$, with $j \in \mathbb{Z}$ for all $t \in \mathbb{R}$,
3. there are two generating functions ϕ and ψ verifying, for all $t \in \mathbb{R}$,

$$\phi(t) = \sum_{k \in \mathbb{Z}} a_k \phi(2t - k) \quad \text{and} \quad \psi(t) = \sum_{k \in \mathbb{Z}} b_k \phi(2t - k) \tag{3.1}$$

   with carefully chosen numerical coefficients (a_k) and (b_k).

This chapter gives some wavelet multiresolution analysis background, an exemple with the Haar wavelet and finishes with a description of the cascade algorithm for computing discrete wavelet transform.

The main references used in this chapter are [33, 46, 38, 45, 49, 50, 48].

3.1 Multiresolution analysis

Multiresolution analysis (MRA) is the analysis under different resolutions, i.e. in different levels of detail and approximation. These different levels of detail and approximations are

obtained by zooming in or zooming out the signal.

Here we study some of the properties of the multiresolution approximations of $L^2(\mathbb{R})$. We show how they relate to wavelet orthonormal bases of $L^2(\mathbb{R})$. We also indicate how the mathematical theory is transformed when it is applied to "discrete" signals.

Definition 3.1.1 (Multiresolution analysis). *Let $(\mathbb{V}_j)_{j\in\mathbb{Z}}$ be a sequence of closed subspaces of $L^2(\mathbb{R})$ and ϕ be a given function of $\mathbb{V}_0$. The sequence of spaces $(\mathbb{V}_j)_{j\in\mathbb{Z}}$ generated by ϕ is termed a **multiresolution analysis (MRA)** if the following properties are verified:*

1. *Nesting: $\mathbb{V}_j \subset \mathbb{V}_{j+1}, \quad j \in \mathbb{Z}$,*
2. *Density: $\bigcup_{j\in\mathbb{Z}} \mathbb{V}_j$ is dense in $L^2(\mathbb{R})$ denotes the closure of the union of vector spaces,*
3. *Separation: $\bigcap_{j\in\mathbb{Z}} \mathbb{V}_j = \{0\}$*
4. *Scaling: $f(\cdot) \in \mathbb{V}_j \Leftrightarrow f(2\cdot) \in \mathbb{V}_{j+1}$, for all $j \in \mathbb{Z}$,*
5. *Complete orthonormality: the integer translates of ϕ , namely $(\phi(\cdot - k))_{k\in\mathbb{Z}}$, form an orthonormal basis of V_0 .*

Let ϕ be a function of $L^2(\mathbb{R})$, such that the sequence $(\phi(\cdot - k))_{k\in\mathbb{Z}}$ is orthonormal. Let $\mathbb{V}_0$ be the subspace of $L^2(\mathbb{R})$ generated by the latter orthonormal sequence.

Define the linear spaces

$$\mathbb{V}_0 = \{f \in L^2(\mathbb{R}) : f(t) = \sum_{k\in\mathbb{Z}} c_k \phi(t-k) \quad \text{and} \quad \sum_{k\in\mathbb{Z}} |c_k|^2 < \infty\}.$$

From $\mathbb{V}_0$ one can generate a sequence of spaces

$$\mathbb{V}_j = \{g(t) = f(2^j t) : f \in \mathbb{V}_0\}, \ j \in \mathbb{Z}$$

Assume that $((\mathbb{V}_j)_{j\in\mathbb{Z}}, \phi)$ is a multiresolution analysis of $L^2(\mathbb{R})$ the subspaces $\mathbb{V}_j$ are nested in the following manner:

$$\mathbb{V}_j \subset \mathbb{V}_{j+1}, \quad j \in \mathbb{Z}.$$

And

$$\bigcup_{j\in\mathbb{Z}} \mathbb{V}_j \text{ is dense in } L^2(\mathbb{R})$$

Then, we can write

$$\mathbb{V}_{j+1} = \mathbb{V}_j \oplus \mathbb{W}_j, \tag{3.2}$$

where $\mathbb{W}_j$ is a subspace orthogonal to $\mathbb{V}_j$. We can continue the decomposition of $\mathbb{V}_j$ up to $\mathbb{V}_0$ and obtain

$$V_{j+1} = V_0 \oplus \bigoplus_{k\in\mathbb{Z}} W_k. \tag{3.3}$$

With the nesting and density properties of MRA we have

$$\bigvee_{j\in\mathbb{Z}} \mathbb{V}_j = \mathbb{V}_0 \oplus \bigoplus_{j\in\mathbb{Z}} \mathbb{W}_j = L^2(\mathbb{R}). \tag{3.4}$$

which means that any function $f \in L^2(\mathbb{R})$ can be represented as a series:

$$f(t) = \sum_{k\in\mathbb{Z}} \alpha_k \phi_{0k}(t) + \sum_{j\in\mathbb{Z}} \sum_{k\in\mathbb{Z}} \beta_{jk}\psi_{jk}(t), \tag{3.5}$$

where α_k, β_{jk} are some coefficients, respectively called scaling (or approximation) and wavelet (or detail) coefficients.

The relation 3.5 is called multiresolution expension of f. It is also called wavelet expension when $(\phi_{jk})_{k\in\mathbb{Z}}$ is a basis for $\mathbb{V}_j$ and $(\psi_{jk})_{k\in\mathbb{Z}}$ is a basis for $\mathbb{W}_j$.

Definition 3.1.2. *Let the sequence of spaces $(\mathbb{V}_j)_{j\in\mathbb{Z}}$ generated by ϕ be a multiresolution analysis of $L^2(\mathbb{Z})$. ϕ is called the father wavelet.*

Definition 3.1.3. *Let $\psi \in \mathbb{W}_0$ a function such that $\{\psi_{0k}(t) = \psi(\cdot - k),\ k \in \mathbb{Z}\}$ is an orthonormal basis of $\mathbb{W}_0$. ψ is called the mother wavelet.*

In relation 3.5, $\mathbb{V}_0$ is the reference space, it is not unique and can be chosen as $\mathbb{V}_{j_0}$, for some $j_0 \in \mathbb{Z}$. The multiresolution decomposion expressed by 3.5 could be limited to V_{j_0} for some $j_0 > 0$ thus the resulted wavelet expension would be:

$$f(x) = \sum_{k\in\mathbb{Z}} \alpha_{j_0k}\phi_{j_0k}(x) + \sum_{j=j_0}^{\infty} \sum_{k\in\mathbb{Z}} \beta_{jk}\psi_{jk}(x), \tag{3.6}$$

The part of the function expressed with the scaling coefficients is called approximation part and the one expressed with the wavelet coefficient, the detail part. The indice j in the wavelet coefficients β_{jk} denotes the resolution level j. The term "resolution level j" is also employed to designate the level of wavelet expansion of a signal f.

Is there a relation between the father and the mother wavelet?

Lemma 3.1.4. *Let $f \in L^2(\mathbb{R})$ and denote by $\hat{f}$ its L^2 Fourier transform. The sequence $(f(\cdot - k))_{k\in\mathbb{Z}}$ is orthonormal if and only if $\sum_{n\in\mathbb{Z}} |\hat{f}(\tau + 2n\pi)|^2 = 1$ for almost all τ.*

Proof: [⇒] Suppose $(f(\cdot - k))_{k\in\mathbb{Z}}$ is orthonormal, hence, on recalling that $\widehat{f(\cdot - k)}(\tau) = \hat{f}(\tau)\exp(-ik\tau)$, we have, for all $k \in \mathbb{Z}$,

$$\begin{aligned}
\delta_{0,k} &= \langle f | f(\cdot - k)\rangle \\
&= \frac{1}{2\pi}\langle \hat{f} | \widehat{f(\cdot - k)}\rangle \text{ by Plancherel's formula} \\
&= \frac{1}{2\pi}\int_{\mathbb{R}} |\hat{f}(\tau)|^2 \exp(-ik\tau)d\tau \\
&= \frac{1}{2\pi}\sum_{n\in\mathbb{Z}}\int_{[2n\pi,2(n+1)\pi[} |\hat{f}(\tau)|^2 \exp(-ik\tau)d\tau \\
&= \frac{1}{2\pi}\Big(\sum_{n\in\mathbb{Z}}\int_{[0,2\pi[} |\hat{f}(\tau + 2n\pi)|^2\Big)\exp(-ik\tau)d\tau.
\end{aligned}$$

Hence all but the 0-th Fourier coefficients of the 2π-periodic function

$$\sum_{n\in\mathbb{Z}} |\hat{f}(\tau + 2n\pi)|^2 \tag{3.7}$$

vanish. Therefore, $\sum_{n\in\mathbb{Z}} |\hat{f}(\tau + 2n\pi)|^2 = 1$.

[⇐] The converse is obtained by reversing the steps of the above reasoning. □

Corollary 3.1.5. *Let ϕ be the scaling function of a multiresolution analysis $((\mathbb{V}_j)_{j\in\mathbb{Z}}, \phi)$. Then $\sum_{n\in\mathbb{Z}} |\hat{\phi}(\tau + 2n\pi)|^2 = 1$.*

Proof: Obvious since $(\phi(\cdot - k))_{k\in\mathbb{Z}}$ is an orthonormal basis of $\mathbb{V}_0$. □

Proposition 3.1.6. *Let $((\mathbb{V}_j)_{j\in\mathbb{Z}}, \phi)$ be a multiresolution analysis. The sequence of closed subspaces $(\mathbb{V}_j)_{j\in\mathbb{Z}}$ of $\mathbb{L}^2(\mathbb{R})$ are nested, $\mathbb{V}_j \subset \mathbb{V}_{j+1}$, if and only if there exists a 2π-periodic function $m_0(\tau), m_0 \in L^2(0, 2\pi)$, such that*

$$\hat{\phi}(\tau) = m_0(\tau/2)\hat{\phi}(\tau/2) \tag{3.8}$$

Proof of this proposition is as follows: it suffices to do it for $j = 0$. For other $j \in \mathbb{Z}$, the proof comes from property 4 of definition 3.1.1.

[⇒] Assume that $\mathbb{V}_0 \subset \mathbb{V}_1$. Hence, $\phi \in \mathbb{V}_1$. By definition, the system $\sqrt{2}\phi(2x - k)$ is a basis in $\mathbb{V}_1$. Therefore, there exists a sequence h_k, such that

$$\phi(t) = \sqrt{2}\sum_{k\in\mathbb{Z}} h_k\phi(2t - k), \tag{3.9}$$

$$h_k = \sqrt{2}\int_{\mathbb{R}} \phi(t)\overline{\phi(2t-k)}dt, \sum_{k\in\mathbb{Z}} |h_k|^2 < \infty$$

By taking the Fourier transform of both sides 3.9 we obtain

$$\hat{\phi}(\tau) = \frac{1}{\sqrt{2}}\sum_{k\in\mathbb{Z}} h_k \exp(-i\tau k/2)\hat{\phi}(\tau/2) = m_0(\tau/2)\hat{\phi}(\tau/2) \tag{3.10}$$

where

$$m_0(\tau) = \frac{1}{\sqrt{2}}\sum_{k\in\mathbb{Z}} h_k \exp(-i\tau k).$$

[$\Leftarrow$] begins with the following lemma.

Lemma 3.1.7. *Let the sequence $(\phi(\cdot - k))_{k\in\mathbb{Z}}$ be orthonormal. Every 2π-periodic function m_0 satisfying 3.8 such that $m_0 \in L^2(0, 2\pi)$, also satisfies*

$$|m_0(\tau)|^2 + |m_0(\tau+\pi)|^2 = 1$$

Proof: With 3.8

$$|\hat{\phi}(2\tau + 2\pi k)^2| = |m_0(\tau + \pi k)|^2 |\hat{\phi}(\tau + \pi k)|^2.$$

Summing up in k and using the fact that the sequence $(\phi(\cdot - k))_{k\in\mathbb{Z}}$ be orthonormal and m_0 is 2π-periodic we get by Corollary 3.1.5 that

$$\begin{aligned}
1 &= \sum_{k\in\mathbb{Z}} |m_0(\tau+\pi k)|^2 |\hat{\phi}(\tau+\pi k)|^2 \\
&= \sum_{l\in\mathbb{Z}} |m_0(\tau+2\pi l)|^2 |\hat{\phi}(\tau+2\pi l)|^2 \\
&= \sum_{l\in\mathbb{Z}} |m_0(\tau+2\pi l+\pi)|^2 |\hat{\phi}(\tau+2\pi l+\pi)|^2 \\
&= \sum_{l\in\mathbb{Z}} |\hat{\phi}(\tau+2\pi l)|^2 |m_0(\tau)|^2 + \sum_{l\in\mathbb{Z}} |\hat{\phi}(\tau+2\pi l+\pi)|^2 |m_0(\tau+\pi)|^2 \\
&= |m_0(\tau)| + |m_0(\tau+\pi)|.
\end{aligned}$$

□

This lemma shows that such function m_0 is bounded. Let $\mathbb{V}_0$ (respectively $\mathbb{V}_1$) be the set of Fourier transforms of the functions of $\mathbb{V}_0$ (respectively $\mathbb{V}_1$) with the previous lemma we obtain:

$$\hat{\mathbb{V}}_0 = \{m(\tau)\hat{\phi}(\tau) : m(\tau)\ 2\pi\text{-periodic}, m \in L^2(0, 2\pi)\},$$
$$\hat{\mathbb{V}}_1 = \{m(\tau/2)\hat{\phi}(\tau/2) : m(\tau)\ 2\pi\text{-periodic}, m \in L^2(0, 2\pi)\},$$

It turns out with proposition 3.8 that every function in $\mathbb{V}_0$ is of the form $m(\tau)m_0(\tau/2)\hat{\phi}(\tau/2)$. Because $m \in L^2(0, 2\pi)$ and m_0 is bounded $m(2\tau)m_0(\tau)$ is a 2π-periodic function belonging to $L^2(0, 2\pi)$.

Lemma 3.1.8. *Let ϕ be a father wavelet which generates a MRA of $L^2(\mathbb{R})$ and let $m_0(\tau)$ be a solution of 3.8. Then the inverse Fourier transform ψ of*

$$\hat{\psi}(\tau) = m_1(\tau/2)\hat{\phi}(\tau/2), \tag{3.11}$$

where $m_1(\tau) = \overline{m_0(\tau + \pi)}\exp(-i\tau)$, is a mother wavelet.

Proof: □

Prove the sequence $(\psi_{0k} = \psi(\cdot - k))_{k\in\mathbb{Z}}$ is orthonormal, i.e

$$\sum_{n\in\mathbb{Z}} |\hat{\psi}(\tau + 2n\pi)|^2 = 1.$$

by lemma 3.1.4.

$$\begin{aligned}
\sum_{n\in\mathbb{Z}} |\hat{\psi}(\tau + 2n\pi)|^2 &= \sum_{k\in\mathbb{Z}} |m_1(\tau/2 + \pi k)|^2 |\hat{\phi}(\tau/2 + \pi k)|^2 \\
&= \sum_{k\in\mathbb{Z}} |m_0(\tau/2 + \pi + \pi k)|^2 |\hat{\phi}(\tau/2 + \pi k)|^2 \\
&= \sum_{l\in\mathbb{Z}} |m_0(\tau/2 + \pi + 2\pi l + \pi)|^2 |\hat{\phi}(\tau/2 + 2\pi l + \pi)|^2 \\
&\quad + \sum_{l\in\mathbb{Z}} |m_0(\tau/2 + \pi + 2\pi l)|^2 |\hat{\phi}(\tau/2 + 2\pi l)|^2 \\
&= \sum_{k\in\mathbb{Z}} |\hat{\phi}(\tau/2 + 2\pi k)|^2 = 1.
\end{aligned}$$

Prove ψ_{0k} is orthogonal to ϕ_{0k}, i.e.

$$\int_{\mathbb{R}} \phi(t - k)\overline{\psi(t - l)}dt = 0, \quad \forall k, l \in \mathbb{Z}$$

i.e,

$$\int_{\mathbb{R}} \phi(t)\overline{\psi(t - k)}dt = 0, \quad \forall k \in \mathbb{Z},$$

denote $\tilde{\psi}(x) = \overline{\psi(-x)}$, and

$$g(k) = \int_{\mathbb{R}} \phi(t)\overline{\psi(t - k)}dt = \int_{\mathbb{R}} \phi(t)\tilde{\psi}(k - t)dt = \phi * \tilde{\psi}(k), \quad \forall k \in \mathbb{Z}.$$

Let $\hat{g}$ be the Fourier transform of g. With Poisson summation formula, the Fourier coefficients of the function $S = \sum_{k\in\mathbb{Z}} \hat{g}(\tau + 2\pi k)$ are $\mathcal{F}^{-1}[\hat{g}](-k) = g(-k), k \in \mathbb{Z}$.
$g(k) = 0, \forall k$ is equivalent to $S(\tau) = 0$ which means

$$\sum_{k\in\mathbb{Z}} \hat{\phi}(\tau + 2\pi k)\overline{\hat{\psi}(\tau + 2\pi k)} = 0.$$

But

$$\begin{aligned}
\sum_{k\in\mathbb{Z}} \hat{\phi}(\tau + 2\pi k)\overline{\hat{\psi}(\tau + 2\pi k)} &= \sum_{k\in\mathbb{Z}} \hat{\phi}(\tau/2 + \pi k)m_0(\tau/2 + \pi k)\overline{\hat{\phi}(\tau/2 + \pi k)m_1(\tau/2 + \pi k)} \\
&= \sum_{k\in\mathbb{Z}} |\hat{\phi}(\tau/2 + \pi k)|^2 m_0(\tau/2 + \pi k)\overline{m_1(\tau/2 + \pi k)} \\
&= m_0(\tau/2)\overline{m_1(\tau/2)} + m_0(\tau/2 + \pi)\overline{m_1(\tau/2 + \pi)} \\
&= m_0(\tau/2)\overline{m_1(\tau/2)} + m_0(\tau/2 + \pi)\overline{m_1(\tau/2 + \pi)}
\end{aligned}$$

Since

$$\begin{aligned}
&m_0(\tau)\overline{m_1(\tau)} + m_0(\tau + \pi)\overline{m_1(\tau + \pi)} = \\
&\qquad m_0(\tau)m_0(\tau + \pi)\exp(i\pi) + m_0(\tau + \pi)m_0(\tau)\exp(i\pi + i\tau) = 0,
\end{aligned}$$

then

$\sum_{k\in\mathbb{Z}} \hat{\phi}(\tau + 2\pi k)\overline{\hat{\psi}(\tau + 2\pi k)} = 0$

Prove that any function f from $\mathbb{V}_1$ has a unique representation.
By definition of $\mathbb{V}_1$, $\{\phi_{1k} = \sqrt{2}\phi(2\cdot - k), \quad k \in \mathbb{Z}\}$ is an orthonormal basis of $\mathbb{V}_1$.
Then

$$f(t) = \sqrt{2}\sum_{k\in\mathbb{Z}} c_k\phi(2t - k),$$

taking the Fourier transform of both sides gives

$$\hat{f}(\tau) = c(\tau/2)\hat{\phi}(\tau/2) \tag{3.12}$$

where

$$c(\tau) = \frac{1}{\sqrt{2}}\sum_{k\in\mathbb{Z}} c_k \exp(-i\tau k).$$

With 3.8

$$\overline{m_0(\tau/2)}\hat{\phi}(\tau) = |m_0(\tau/2)|^2\hat{\phi}(\tau/2),$$

and with 3.11

$$\overline{m_1(\tau/2)}\hat{\psi}(\tau) = |m_1(\tau/2)|^2\hat{\phi}(\tau/2),$$

By summing up the two previous equations we obtain:

$$\hat{\phi}(\tau/2)\left[|m_0(\tau/2)|^2 + |m_1(\tau/2)|^2\right] = \overline{m_0(\tau/2)}\hat{\phi}(\tau) + \overline{m_1(\tau/2)}\hat{\psi}(\tau) \tag{3.13}$$

Considering lemma 3.11 and lemma 3.1.7 yields

$$|m_0(\tau/2)|^2 + |m_1(\tau/2)|^2 = |m_0(\tau/2)|^2 + |m_0(\tau/2+\pi)|^2 = 1,$$

thus equation 3.13 becomes

$$\hat{\phi}(\tau/2) = \overline{m_0(\tau/2)}\hat{\phi}(\tau) + \overline{m_1(\tau/2)}\hat{\psi}(\tau),$$

and equation 3.1.7

$$\hat{f}(\tau) = c(\tau/2)\overline{m_0(\tau/2)}\hat{\phi}(\tau) + c(\tau/2)\overline{m_1(\tau/2)}\hat{\psi}(\tau).$$

Thus in the time domain, f has a unique representation in $\mathbb{V}_0 \oplus \mathbb{W}_0$. It's now proven that $\{\psi_{0k}(t) = \psi(\cdot - k),\ k \in \mathbb{Z}\}$ is an orthonormal basis of $\mathbb{W}_0$.

Finally the relation between the father and mother wavelet is given by the following lemma.

Lemma 3.1.9. *The mother wavelet satisfies*

$$\psi(t) = \sqrt{2}\sum_{k\in\mathbb{Z}} \lambda_k \phi(2t-k), \tag{3.14}$$

where $\lambda_k = (-1)^{k+1}\bar{h}_{1-k}$*, and* h_k *coefficients in the relation satisfied by the father wavelet*

$$\phi(t) = \sqrt{2}\sum_{k\in\mathbb{Z}} h_k \phi(2t-k). \tag{3.15}$$

Proof: We know that

$$m_0(\tau) = \frac{1}{\sqrt{2}}\sum_{k\in\mathbb{Z}} h_k \exp(-i\tau k)$$

then

$$\begin{aligned}
\overline{m_0(\tau/2+\pi)} &= \overline{\frac{1}{\sqrt{2}}\sum_{k\in\mathbb{Z}} h_k \exp(-ik(\tau/2+\pi))} \\
&= \frac{1}{\sqrt{2}}\sum_{k\in\mathbb{Z}} \bar{h}_k \exp(ik(\tau/2+\pi)) \\
&= \frac{1}{\sqrt{2}}\sum_{k\in\mathbb{Z}} \bar{h}_k (-1)^k \exp(ik\tau/2).
\end{aligned}$$

With lemma 3.11

$$\begin{aligned}
\hat{\psi}(\tau) &= \overline{m_0(\tau/2+\pi)}\exp(-i\tau/2)\hat{\phi}(\tau/2) \\
&= \frac{1}{\sqrt{2}}\sum_{k\in\mathbb{Z}}\bar{h}_k(-1)^k\exp(ik\tau/2)\exp(-i\tau/2)\hat{\phi}(\tau/2) \\
&= \frac{1}{\sqrt{2}}\sum_{k\in\mathbb{Z}}\bar{h}_k(-1)^k\exp(i(k-1)\tau/2)\hat{\phi}(\tau/2) \\
&= \frac{1}{\sqrt{2}}\sum_{k'\in\mathbb{Z}}\bar{h}_{1-k'}(-1)^{k'+1}\exp(-ik'\tau/2)\hat{\phi}(\tau/2) \quad \text{avec} \quad k'=1-k \\
&= \sqrt{2}\sum_{k\in\mathbb{Z}}\lambda_k\exp(-ik\tau/2)\frac{1}{2}\hat{\phi}(\tau/2)
\end{aligned}$$

By taking the inverse Fourier transform of both sides we obtain relation 3.14

□

3.2 The Haar wavelet

The Haar wavelet was the first wavelet to have been constructed [39, 40, 41], some 70 years before the theory of wavelets was established [42, 43, 44, 46, 47] and the very term **wavelet** coined. Its simplicity renders it particularly instructive to establish the main properties of this wavelet as a warming up of the general theory. We follow §7.1 of [33].

Example 3.2.1 (**The Haar multiresolution**). *Let $\phi \in L^2(\mathbb{R})$ be defined by $\phi(t) = \mathbb{1}_{[0,1[}(t)$ and*

$$\mathbb{V}_0 = \overline{\mathsf{span}}\{\phi(\cdot - k), k \in \mathbb{Z}\} \tag{3.16}$$

The nested sequence of closed subspaces is defined either form V_0 through the scaling property or by introducing the sequence of functions $(\phi)_{j,k\in\mathbb{Z}}$, by $\phi_{j,k}(t) = 2^{j/2}\phi(2^j t - k)$ and defining

$$\mathbb{V}_j = \overline{\mathsf{span}}\{\phi_{j,k}, k \in \mathbb{Z}\}, \forall j \in \mathbb{Z} \tag{3.17}$$

The pair $((\mathbb{V}_j)_{j\in\mathbb{Z}}, \phi)$ is then a multiresolution analysis.

Remark. *Since $\phi := \phi_{0,0} \in \mathbb{V}_0 \subset \mathbb{V}_1$ and $(\phi_{1,k})_{k\in\mathbb{Z}}$ is an orthonormal basis of $\mathbb{V}_1$, it follows that we can expand ϕ in that basis*

$$\phi(t) = \sum_{k\in\mathbb{Z}} c_k \sqrt{2}\phi(2t-k), \text{where } c_k = \langle \phi_{1,k} | \phi \rangle = \sqrt{2} \int_{\mathbb{R}} \bar{\phi}(2t-k)\phi(t)dt. \tag{3.18}$$

For the Haar scaling function $\phi(t) = \mathbb{1}_{[0,1[}(t)$, we have

$$1 = ||\phi||_2^2 = \sum_{k\in\mathbb{Z}} |c_k|^2. \tag{3.19}$$

This relation is obviously verified if the coefficients read

$$c_k = \begin{cases} \frac{1}{\sqrt{2}} & \text{if } k \in \{0,1\} \\ 0 & \text{otherwise} \end{cases} \tag{3.20}$$

(and consequently $a_k = \sqrt{2}c_k$.)

Since the closed subspace $\mathbb{V}_0$ is contained into $\mathbb{V}_1$, we can, by the projection theorem, decompose $\mathbb{V}_1$ into the orthogonal direct sum $\mathbb{V}_1 = \mathbb{V}_0 \oplus \mathbb{W}_0$. More generally, the decomposition holds for all subspaces of the nested sequence.

Definition 3.2.2. *Let*

$$\mathbb{V}_{j+1} = \mathbb{V}_j \oplus \mathbb{W}_j, \forall j \in \mathbb{Z} \tag{3.21}$$

*where $\mathbb{W}_j$ is the orthogonal complement $V_j^{\perp_{\mathbb{V}_{j+1}}}$ of $\mathbb{V}_j$ in $\mathbb{V}_j+1$. The spaces $(\mathbb{W}_j)_{j\in\mathbb{Z}}$ are termed **detail** or **wavelet spaces**. A function $\psi \in \mathbb{W}_0$ such that the sequence $(\psi(\cdot - k), k \in \mathbb{Z})$ provide an orthonormal basis of $\mathbb{W}_0$ is termed a **mother wavelet**.*

It is then obvious that

$$L^2(\mathbb{R}) = \mathbb{V}_0 \oplus (\oplus_{k\in\mathbb{N}} \mathbb{W}_n) \text{ and } \mathbb{V}_0 = \oplus_{k=1}^{\infty} \mathbb{W}_{-k}. \tag{3.22}$$

The main characteristic of the the multiresolution analysis is the fact that the bases of the spaces $\mathbb{V}_j$, **for all** $j \in \mathbb{Z}$, are constructed from a common **universal scaling function** ϕ by repeated scaling and translation transformations. The wavelets are the pendant of the bases of spaces $\mathbb{W}_j$, constructed **for all** $j \in \mathbb{Z}$ from repeated scaling and translation of a common **universal mother wavelet function** ψ.

Example 3.2.3 (The Haar mother wavelet). *Let $\psi(t) = \phi(2t) - \phi(2t-1)$. Obviously $\phi \in \mathbb{V}_1$ and $\psi \perp \phi$. More generally, we see that $\psi \perp \phi_{0,k} = \phi(\cdot - k)$ for all $k \in \mathbb{Z}$, hence $\psi \in \mathbb{V}_0^{\perp \mathbb{V}_1} = \mathbb{W}_0$. It is immediate to show that*

$$\overline{\mathsf{span}}\{\psi(\cdot - k), k \in \mathbb{Z}\} = \mathbb{W}_0. \tag{3.23}$$

Consequently, on introducing $\psi_{j,k}(t) = 2^{j/2}\psi(2^j t - k)$, for $j, k \in \mathbb{Z}$, we see, by scaling and translation, that

$$\overline{\mathsf{span}}\{\psi_{j,k}, k \in \mathbb{Z}\} = \mathbb{W}_j, \forall j \in \mathbb{Z} \text{ and } \overline{\mathsf{span}}\{\psi_{j,k}, j, k \in \mathbb{Z}\} = L^2(\mathbb{R}). \tag{3.24}$$

Remark. *The family $(\psi_{j,k})_k$ constitute an orthonormal basis of $\mathbb{W}_j$ and $(\psi_{j,k})_{j,k}$ an orthonormal basis of $L^2(\mathbb{R})$. It is also immediate to check that the particular functions ϕ and ψ intervening in the definition of the Haar wavelets verify the conditions*

$$\phi(t) = \sum_{k \in \mathbb{Z}} a_k \phi(2t - k), \quad \text{(scaling equation)} \tag{3.25}$$

$$\psi(t) = \sum_{k \in \mathbb{Z}} b_k \phi(2t - k), \quad \text{(detail equation)} \tag{3.26}$$

with

$$a_k = \begin{cases} 1 & \text{if } k \in \{0, 1\} \\ 0 & \text{otherwise,} \end{cases} \tag{3.27}$$

$$a_k = \begin{cases} 1 & \text{if } k = 0, \\ -1 & \text{if } k = 1, \\ 0 & \text{otherwise.} \end{cases} \tag{3.28}$$

3.3 The cascade algorithm

Contrary to the Fourier transform where we have only one resolution level, multiresolution analysis have many resolution levels represented by the space $\mathbb{W}_j$. But we often employ the term "resolution level j" to designate the coefficients β_{jk} and the functions ψ_{jk}.

The cascade algorithm or pyramidal algorithm is a framework for computing sequentially the higher level wavelet coefficients from the lower level ones and vice versa. It was

introducted by S. Mallat [49, 50]. The wavelet coefficients of a given function f at a resolution level j are $\alpha_{jk} = \langle f, \phi_{jk} \rangle$ and $\beta_{jk} = \langle f, \psi_{jk} \rangle$, where $\langle \cdot, \cdot \rangle$ denotes the scalar product of the Hilbert space $L^2(\mathbb{R})$.

Define a relation between α_{jk} and $\alpha_{j+1,k}$, two scaling coefficients at two successive resolution levels.

$$\begin{aligned}
\alpha_{jk} &= \langle f, \phi_{jk} \rangle \\
&= \int_{\mathbb{R}} f(t)\phi_{jk}(t)dt \\
&= \int_{\mathbb{R}} f(t)2^{j/2}\phi(2^j t - k)dt \\
&= \int_{\mathbb{R}} f(t)2^{j/2}\sqrt{2}\sum_{s\in\mathbb{Z}} h_s \phi(2(2^j t - k) - s)dt, \qquad \text{with 3.15} \\
&= \int_{\mathbb{R}} f(t)\sum_{l\in\mathbb{Z}} h_{l-2k} 2^{(j+1)/2}\phi(2^{j+1}t - l)dt, \qquad l = 2k + s \\
&= \sum_{l\in\mathbb{Z}} h_{l-2k}\int_{\mathbb{R}} f(t)\phi_{j+1,l}(t)dt \\
&= \sum_{l\in\mathbb{Z}} h_{l-2k}\alpha_{j+1,l} \qquad (3.29)
\end{aligned}$$

Note in previous calculation the relation

$$\phi_{jk}(t) = \sum_{l\in\mathbb{Z}} h_{l-2k}\phi_{j+1,l}(t). \qquad (3.30)$$

The relation between β_{jk} and $\alpha_{j+1,k}$ is obtained with the same step and using 3.14.

$$\beta_{jk} = \sum_{l\in\mathbb{Z}} \lambda_{l-2k}\alpha_{j+1,l} \qquad (3.31)$$

Note also the relation

$$\psi_{jk}(t) = \sum_{l\in\mathbb{Z}} \lambda_{l-2k}\phi_{j+1,l}(t). \qquad (3.32)$$

The cascade algorithm is invertible, we can get higher level wavelet coefficients from lower level ones i.e get $\alpha_{j+1,k}$ from α_{jk} and β_{jk}.

For a given $f \in L^(\mathbb{R})$ consider the orthogonal projection of f on the space $\mathbb{V}_{j+1}$. We know with the orthogonal decomposition that $\mathbb{V}_{j+1} = \mathbb{V}_j \oplus \mathbb{W}_j$. The orthogonal projection

of f on $\mathbb{V}_{j+1}$ can be written as

$$f(t) = \sum_{k\in\mathbb{Z}} \alpha_{jk}\phi_{jk}(t) + \sum_{k\in\mathbb{Z}} \beta_{jk}\psi_{jk}(t)$$

When computing the inner products of $\phi_{j+1,s}$ with both sides of the previous equation we obtain

$$\langle f, \phi_{j+1,s}\rangle = \sum_{k\in\mathbb{Z}} \alpha_{jk}\langle \phi_{jk}, \phi_{j+1,s}\rangle + \sum_{k\in\mathbb{Z}} \beta_{jk}\langle \psi_{jk}, \phi_{j+1,s}\rangle$$

Then with 3.30 and 3.32 we have

$$\begin{aligned} \alpha_{j+1,s} &= \sum_{k\in\mathbb{Z}} \alpha_{jk} \sum_{l\in\mathbb{Z}} h_{l-2k}\langle \phi_{j+1,l}, \phi_{j+1,s}\rangle + \sum_{k\in\mathbb{Z}} \beta_{jk} \sum_{l\in\mathbb{Z}} \lambda_{l-2k}\langle \phi_{j+1,l}, \phi_{j+1,s}\rangle \\ &= \sum_{k\in\mathbb{Z}} h_{s-2k}\alpha_{jk} + \sum_{k\in\mathbb{Z}} \lambda_{s-2k}\beta_{jk} \end{aligned} \tag{3.33}$$

See the following schema for an illustration of the cascade algorithm for the computation of wavelet coefficients of a discrete signal $\mathcal{S}$ with 8 samples $(x_0, , \ ..., \ x_7)$. $\mathcal{S}$ is considered at its highest resolution level i.e level 3, because $8 = 2^3$. Then $x_0 = \alpha_{3,0}$, $x_1 = \alpha_{3,1}$, $x_2 = \alpha_{3,2}$, $x_3 = \alpha_{3,3}$, $x_4 = \alpha_{3,4}$, $x_5 = \alpha_{3,5}$, $x_6 = \alpha_{3,6}$, $x_7 = \alpha_{3,7}$.

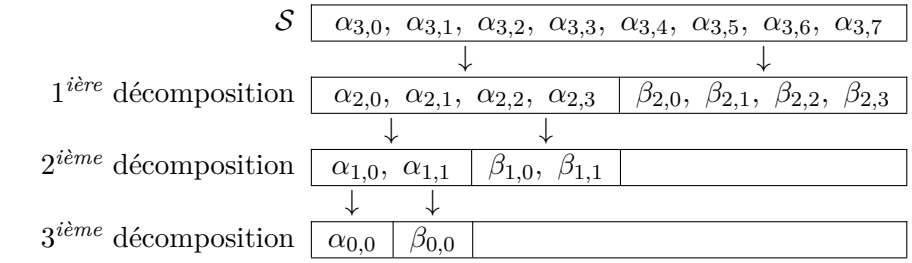

Figure 3.1: Application of the cascace algorithm on a discrete signal with 8 samples

Chapter 4

ECG beat classification using waveform similarity and RR intervals

4.1 Introduction

The electrocardiogram (ECG) is one of the most important tools in the diagnosis of heart diseases. It graphically displays the electrical activity of the heart recorded from electrodes on the body surface [22]. From a plot of an ECG, a cardiologist can analyze the shape of the waveform and determine the nature of the diseases afflicting the heart. Abnormal heart beats in an ECG that correspond to a particuliar disease can be rare and widespread over a long recording, and thus tracking down abnormalities can be tedious. Therefore, it is desirable to develop computer-based diagnosis tools.

Besides noise, the main problem in computer-based classification of heart beats in ECG recordings is the wide variety in the shape of beats belonging to a given class and the similarity in the shape of beats belonging to different classes [1]. Therefore, algorithms for computer-based diagnosis generally have three steps: ECG beat detection, extraction of useful features from beats, and classification. A number of methods have been developed for beat detection [78, 6]. Feature extraction can be done in the time domain [13], in the frequency domain [7], by multiscale decomposition [9], by multifractal analysis [10], or by statistical means [1]. Classification can be performed using neural networks [14, 2], a mixture of experts model [12], or a switchable scheme [15].

Although statistical methods of ECG beat recognition [1, 15, 16] have good recognition

accuracy, Hu [12] suggested that the specificities of each patient's electrocardiogram should be taken into account in ECG beat classification.

In this chapter we introduce an electrocardiogram (ECG) beat classification method based on waveform similarity and RR intervals. The method is a patient-specific and classifies six types of heart beat, namely normal beats, atrial premature beats, paced beats, premature ventricular contractions, left bundle branch block beats, and right bundle branch block beats. The wavelet transform has been used to process non-stationary signals such as ECGs [11]. Therefore, it is employed in this study for ECG signal denoising and reducing the number of samples per beat. A heart beat database containing five classes of annotated beats is created for the classifier. Each time a patient's ECG beats have to be classified, the beats in the first five minutes of the ECG recording are manually annotated and integrated into the heart beat database. The classifier thus learns with each submitted ECG recording. The beats of the patient's ECG are first clustered according to the similarity in the shape of their waveform and then each cluster is classified by considering the greatest similarity of its elements to beats in the classifier heart beat database.

The method presented in this chapter is published in [87].

4.2 ECG signal pre-processing

The ECG is an electrical signal recorded from electrodes placed on the body surface. The ECG signal is analog in nature, therefore its processing begins from the digital electrocardiograph by a sampling. For exemple, ECG records of the MIT/BIH arrhythmia database are digitized at 360 samples per second. The ECG signal is generally corrupted by noise of diverse origin: muscle artifact, electric voltage of the device, breathing, poor contact of electrodes etc. Those noises are responsible of the baseline wander and the high oscillation of low amplitude observed on the electrocardiogram. The baseline wander cancellation is necessary for proper alignment of beats (the PQRST complexe). The baseline wander can cause deformations of the QRS complex and therefore leads to misinterpretation of the ECG. On the other hand, the high frequency low amplitude oscillation in the signal makes difficult the delineation of the different waves (which are useful features for ECG interpretation) composing the heart beat. For all these reasons the ECG must be denoised.

4.2.1 ECG noise reduction techniques

Many denoising techniques are proposed in the literature. There are adaptive scheme methods based on the Least Means Square algorithm (LMS) such as, "The adaptive impluse correlated filter (AICF)" proposed by Thakor an Zhu [64], and "The time-sequenced

adaptive filter (TSAF)" [65] which show good performances but not always. But "The single-input adaptive filter" based on the first two is robust to noise and gives good denoising results [66]. There are also methods based window averaging such as the one proposed by H. SadAbadi [67], but it's not easy to implement. Currently in the ECG denoising area there's a growing interest in methods that use the wavelet transformation. Several recent work based on wavelet transform had shown good denoising results [68, 69, 70, 71]. After the choice of the type of wavelet and the thresholding parameters, the denoising technique was performed by the following steps: do a forward discrete wavelet transform up to some resolution level, do a soft thresholding on the wavelet coefficients and finish with an inverse discrete wavelet transform.

Baseline wander cancellation

The baseline wander is a low frequency noise present in electrocardiograms. Its frequency is usually less than 1Hz but can in exercise ECG be more [72, 73, 64]. We know that approximation or scaling coefficients α_{jk} in the DWT at low resolution levels represent the low frequency part of a signal [46]. Therefore the method of canceling baseline wander using wavelet transform consists of decomposing the noisy signal to a certain low resolution level l_0, to nullify the approximation coefficients at that resolution level and finally to reconstruct the signal to its original resolution level. A summary of the steps is given below:

1. Assume the discrete-time signal $x(t)$ has $N = 2^J$, $(J \in \mathbb{N})$ samples at its highest available resolution (J). Expressing this signal on the basis of scaling function $\{\phi_{Jk},\ k \in \mathbb{Z}\}$ at the resolution level J gives:

$$x(t) = \sum_{k=0}^{N-1} \alpha_{Jk}\phi_{Jk}(t). \tag{4.1}$$

2. The discrete wavelet transform of $x(t)$ to a certain low resolution level $l_0 < J$ is:

$$x(t) = \sum_{k=0}^{2^{l_0}-1} \alpha_{l_0k}\phi_{l_0k}(t) + \sum_{j=l_0}^{J}\sum_{k=0}^{2^j-1} \beta_{jk}\psi_{jk}(t), \tag{4.2}$$

   with $\beta_{Jk} = 0$ for all k because at the resolution level J there is no wavelet coefficient.

3. The cancellation of scaling coefficient at resolution level l_0 which represent the low frequency noise leads to:

$$x'(t) = \sum_{j=l_0}^{J}\sum_{k=0}^{2^j-1} \beta_{jk}\psi_{jk}(t), \tag{4.3}$$

4. The reconstruction of $x'(t)$ to the resolution level J gives the expression of the signal $x(t)$ without the low frequency noise (the baseline wander):

$$x'(t) = \sum_{k=0}^{N-1} \alpha'_{Jk}\phi_{Jk}(t). \tag{4.4}$$

To apply this method one need to investigate the two questions:

1. Which mother wavelet suits better for the discrete wavelet transform in order to get best results?

2. At what resolution level, approximation coefficients should be set to zero?

A. Khawaja [74] founds that the mother wavelet Daubechies11 gives better results than the others namely Symlet12, Symlet10, Daubechies10 and Coiflet5. The approximation coefficient to nullify are found to belong to the signal at the ninth resolution level under the original one. For exemple, if the original signal has 2^{15} samples per lenght unit, it will be decomposed nine times to find the approximation coefficient representing the baseline wander. Figure 4.1 shows the result of the application of the denoising method on a noisy ECG signal.

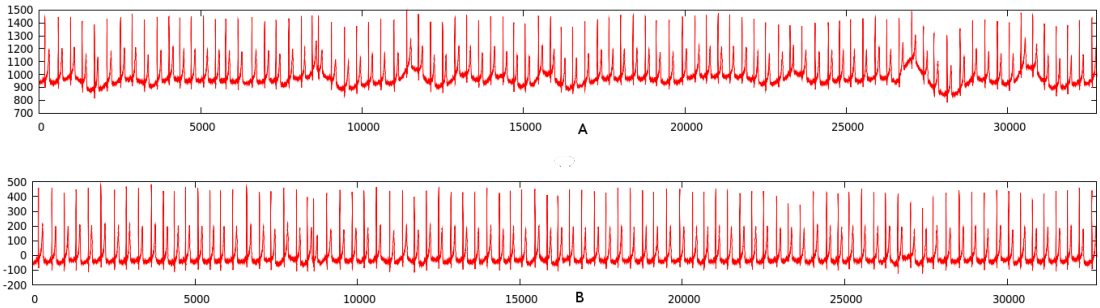

Figure 4.1: Baseline wander cancellation on record number 113, MLII from MIT-Arrhythmia Database: (A) Original signal (B) Denoised signal.

High frequency noise cancellation

The high frequency noise in ECG signals is manifested by the presence of rapid oscillations of low amplitude in the plot. We know that detail or wavelet coefficients β_{jk} in the DWT represent the high frequency part of a signal [46]. Therefore a part of the value of the

details coefficients is responsible for such unwanted oscillations in the ECG signal. Thus two techniques of selection of detail coefficients based on a threshold value are introduced by D.Donoho [75]. These techniques are known as soft thresholding and hard thresholding.

Assume $\{\beta_{jk},\ j,k \in \mathbb{Z}\}$ are detail coefficients of the noisy signal. In the *hard thresholding* one replaces β_{jk} with $\hat{\beta}_{jk}$ defined by:

$$\hat{\beta}_{jk} = \begin{cases} \beta_{jk}, & \text{if } |\beta_{jk}| \geq T_r \\ 0, & \text{if } |\beta_{jk}| < T_r \end{cases} \tag{4.5}$$

where T_r is a certain threshold. In the *soft thresholding* one replaces β_{jk} with $\hat{\beta}_{jk}$ defined by:

$$\hat{\beta}_{jk} = \begin{cases} \mathsf{sign}(\beta_{jk})(|\beta_{jk}| - T_r), & \text{if } |\beta_{jk}| \geq T_r \\ 0, & \text{if } |\beta_{jk}| < T_r \end{cases} \tag{4.6}$$

The value of the threshold T_r is based on some prior information that may exist on the signal. A fixed threshold T_r, is introduced by Donoho and Johnstone in the form:

$$T_r = \sigma\sqrt{2\log(n)} \tag{4.7}$$

where σ is estimated using the median of the absolute deviation of the detail coefficients of the first wavelet decomposition of the signal, and n is their number:

$$\sigma = 1.483 \times \mathsf{median}((\beta_{J-1,k})_{k\in\mathbb{Z}}), \tag{4.8}$$

Let J be the highest resolution level of the signal. Steps of high frequency noise cancellation using *soft thresholding* are:

1. Do the first decomposition of the ECG signal $x(t)$.

$$x(t) = \sum_{k=0}^{2^J-1} \alpha_{Jk}\phi_{Jk}(t). \tag{4.9}$$

   The first decomposition of $x(t)$ gives:

$$x(t) = \sum_{k=0}^{2^{J-1}-1} \alpha_{J-1,k}\phi_{J-1,k}(t) + \sum_{k=0}^{2^{J-1}-1} \beta_{J-1,k}\psi_{J-1,k}(t), \tag{4.10}$$

   Compute σ from $\beta_{J-1,k\ k\in\mathbb{Z}}$ and T_r from equation 4.7.

2. Compute the complete discrete wavelet decomposition of the signal. The expression of $x(t)$ becomes:

$$x(t) = \alpha_{00}\phi_{00}(t) + \sum_{j=0}^{J}\sum_{k=0}^{2^j-1} \beta_{jk}\psi_{jk}(t) \tag{4.11}$$

Replace all the detail coefficients β_{jk} with $\hat{\beta}_{jk}$ (equation 4.6). We obtain the new signal $\hat{x}(t)$:

$$\hat{x}(t) = \alpha_{00}\phi_{00}(t) + \sum_{j=0}^{J}\sum_{k=0}^{2^j-1}\hat{\beta}_{jk}\psi_{jk}(t), \tag{4.12}$$

3. Compute the inverse discrete wavelet transform of $\hat{x}(t)$ to obtain the denoised signal corresponding to the original signal $x(t)$:

$$\hat{x}(t) = \sum_{k=0}^{2^J-1}\hat{\alpha}_{Jk}\phi_{Jk}(t). \tag{4.13}$$

Experimental results obtained in [69] have revealed that Daubechies mother wavelet of order 8 gives better results for high frequency noise cancellation than Symlets or Coiflets. Figure 4.2 shows the result of the application of the denoising method on a noisy ECG signal.

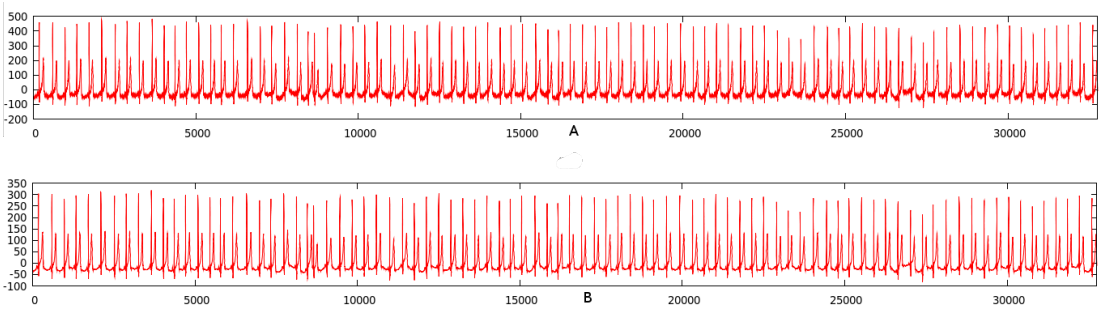

Figure 4.2: High frequency noise cancellation on record number 113, MLII from MIT-Arrhythmia Database: (A) Original signal (B) Denoised signal.

Figure 4.3 shows the application of the two denoising techniques (baseline wander cancellation and high frequency noise cancellation) on a noisy ECG signal.

4.3 Proposed method

4.3.1 Feature extraction

The morphology of the QRS complex and the instantaneous RR interval (the interval between two successive R peaks) play important roles in heart disease diagnosis [15, 16].

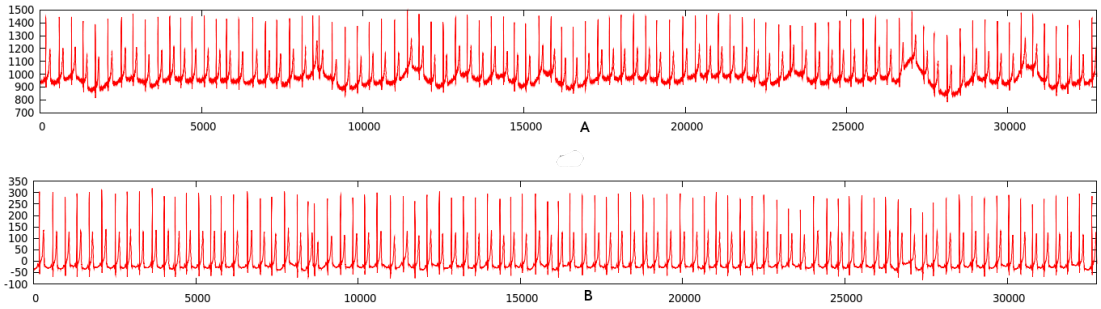

Figure 4.3: Full noise cancellation on record number 113, MLII from MIT-Arrhythmia Database: (A) Original signal (B) Denoised signal.

For the classification of an ECG beat, the ratio of the RR interval before the beat to that after it is a useful feature. For NBs, LBBBs, RBBBs, and PBs, this ratio is near or equal to 1, and for APBs and PVCs, this ratio is less than 1. If PVCs or APBs occur in groups [22], this ratio can be near or equal to 1 but the RR interval will be very small compared to the mean RR between non-premature beats (heart beats that do not occur earlier than expected) in the ECG signal.

The distinction between PVCs and APBs is that a PVC is usually followed by a compensatory pause, i.e., the RR interval between two QRS enclosing a PVC is twice the normal RR interval; in contrast, a APB is rarely followed by a compensatory pause, i.e., the RR interval between two QRS enclosing a APB is less than twice the normal RR interval [22].

RR_b, RR_a (respectively the RR intervals before and after the R peak) along with RR_m (the mean RR between non-premature beats) are considered as features in this study. The R peaks are taken from the annotation files of the MIT-BIH arrhythmia database.

From the ECG recording, beats are extracted using 128 sampling points centered at the R peak. The number of samples per beat is reduced to 16 by the discrete wavelet transform as follows. With the multiresolution approach, at resolution level j_0, the beat with 128 points is denoted as:

$$b_{128}(t) = \sum_{k=0}^{2^{j_0}-1} \alpha_{j_0 k}\phi_{j_0 k}(t), \qquad \beta_{j_0 k} = 0, \tag{4.14}$$

The decomposition to resolution level $j_0 - 3$ is:

$$b_{128}(t) = \sum_{k=0}^{2^{j_0-3}-1} \alpha_{j_0-3,k}\phi_{j_0-3,k}(t) + \sum_{j=j_0-3}^{j_0} \sum_{k=0}^{2^j-1} \beta_{jk}\psi_{jk}(t), \tag{4.15}$$

where ϕ and ψ are scaling functions and wavelet functions at the corresponding resolution level, respectively. The beats at resolution level j_0 can be characterized by $2^{j_0} = 128$ samples per length unit. With $j_0 = 7$, Eq. (5) becomes:

$$b_{128}(t) = \sum_{k=0}^{2^4-1} \alpha_{4,k}\phi_{4,k}(t) + \sum_{j=4}^{7} \sum_{k=0}^{2^j-1} \beta_{jk}\psi_{jk}(t) \tag{4.16}$$

By setting all the coefficients β_{jk} to zero, the beat with 16 points is:

$$z(t) := b_{16}(t) = \sum_{k=0}^{2^4-1} \alpha_{4,k}\phi_{4,k}(t) \tag{4.17}$$

Reducing the number of samples per beat from 128 to 16 reduces the amount of required memory and accelerates the processing. Figure 4.4 gives different level of approximation of a heart beat. When the length reduction goes further (less then 16 samples) the heart beat is so distorted that it no longer resembles a beat.

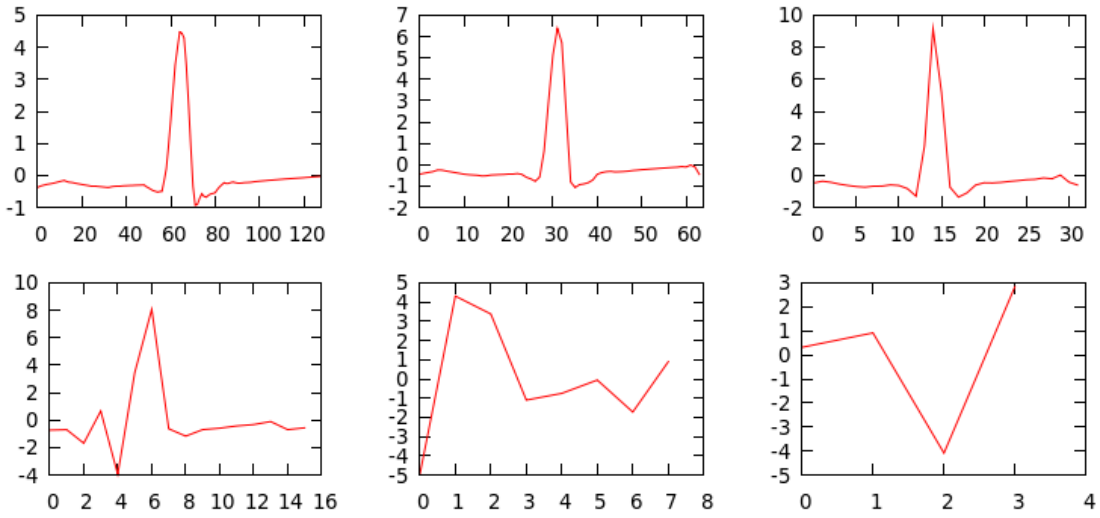

Figure 4.4: Different level of approximation of a heart beat from signal 113, MLII of MIT-Arrhythmia Database.

4.3.2 Similarity function

Let $\mathbb{A}$ be the orthonormal family of scaling functions $\{\phi_{4,k}\}$ at resolution level 2^4. From Eq. 4.17, $\mathbb{A}$ generates a vector space $\mathbb{B} \subset L_2(\mathbb{R})$ containing all the beats. Therefore, the scalar product in $L_2(\mathbb{R})$ can also be defined for every two vectors of $\mathbb{B}$, $|\Psi\rangle = \sum_{\phi\in\mathbb{A}} \Psi_\phi|\phi\rangle$ and $|\Psi'\rangle = \sum_{\phi\in\mathbb{A}} \Psi'_\phi|\phi\rangle$, by $\langle\Psi|\Psi'\rangle = \sum_{\phi\in\mathbb{A}} \overline{\Psi}_\phi\Psi'_\phi$, where $\overline{\Psi}_\phi$ denotes the complex conjugate of Ψ_ϕ (it coincides with Ψ_ϕ if it is real). A similarity function on $\mathbb{B}$ is defined as follows:

$$\sigma\colon \mathbb{B}\times\mathbb{B} \to [0,1], \qquad \sigma(\Psi,\Psi') = \frac{\langle\Psi|\Psi'\rangle}{\|\Psi\|\cdot\|\Psi'\|} \tag{4.18}$$

where $\|\cdot\|$ denotes a Hilbert norm on $\mathbb{B}$. The similarity function indicates the degree of proximity in the shape of two beats. Such similarity function have been used previously see [51].

4.3.3 Clustering algorithm

Let $S = \{z_1(\cdot), z_2(\cdot), \cdots, z_n(\cdot)\}$ be a set of heart beats. S can be partitionned into k clusters ($k \leq n$) $S = S_1 \cup S_2 \cup \cdots \cup S_k$ so that beats in the same cluster are more similar in the shape to each other then to those belonging the other clusters.

The clustering algorithm proceeds by iterating the following step:
Choose at random $c_i \in S - \bigcup_{j<i} S_j$, c_i will be the centroid of S_i, $1 \leq i \leq k$.

$$S_i = \{x \in S - \bigcup_{j<i} S_j : r \leq \sigma(c_i, x) \leq 1\}$$

where σ is the similarity function described in equation 4.18, and r the mimimum degree of similarity.
The process will stops when there is no element left in the $S - \bigcup_{j<i} S_j$ i.e $S - \bigcup_{j<i} S_j = \emptyset$. This clustering algorithm is easy to implement and runs in $O(n^2)$ operations. Some other clustering algorithms commonly used in statistical data analysis are presented in [51].

4.3.4 Classification

As stated in [55], computer analysis cannot substitute a physician's interpretation of ECG. Therefore, the proposed classifier uses a database of known beats (reduced version of the original 128-samples-per-beat data) taken within the first five minutes of each recording in the MIT/BIH arrhythmia database. The classifier heart beat database contains five

classes of beat, namely NBs, LBBBs, RBBBs, PBs, and PVCs. The APB type is not in the database because APBs can be similar to NBs, LBBBs, and RBBBs, and thus their identification is mainly based on the RRb/RRa ratio. The heart beat database is updated each time a patient's ECG recording is examined. This practice conforms to the American Association of Medical Instrumentation recommended procedure, which allows the first five minutes of data in an ECG recording to be used to fine-tune the classifier [12]. After the denoising step, the classification of a patient's ECG recording is done as follows:

(1) Beats are extracted using 128 samples per beat centered at the R peak. For each beat, the RR intervals before (RR_b) and after (RR_a) its R peak are taken. The number of samples per beat is then reduced to 16 using discrete wavelet decomposition. The resulting beat is normalized to reduce waveform differences in a given class by subtracting the mean value and then dividing the result by the standard deviation [15].

(2) The beats within the first five minutes of the ECG recording are added to the classifier beat database. The mean RR (RR_m) of beats in those 5 minutes is taken as a feature.

(3) The beats in the 25 remaining minutes are hierarchically clustered by similarity before classification.

(4) The class of a beat is identified using its highest similarity to beats in the classifier database.

(5) 1)If the class is found to be NB, LBBB, or RBBB, the ratio RR_b/RR_a is calculated. If $RR_b/RR_a < (1 - \epsilon_1)$ or $(RR_a + RR_b) < (2RR_m - \epsilon_2)$, then the class is changed to APB; otherwise, the class is unchanged. The optimal ϵ_1 and ϵ_2 values are identified from experiments.

(6) The class of a cluster is the class of the element which has the highest similarity to a beat in the classifier ECG database.

4.4 Results and discussion

The classifier was tested with 25 minutes of data from each 30-minute ECG recording in the MIT/BIH arrhythmia database. The first five minutes of the ECG recordings was used to build the heart beat database for the classifier. In each ECG recording used in this study, only beats in the NB, LBBB, RBBB, APB, PVC, and PB classes were considered. The RR intervals were calculated from the position of the R peak documented in the annotation files of the MIT/BIH database. The mean RR (RR_m) used in the identification of APBs was calculated using the first five minutes of the signal. For the clustering of beats before

classification, two beats belonged to the same cluster if their similarity was greater or equal to 0.95.

The performance of the classifier was evaluated in terms of the accuracy rate per ECG signal, the overall accuracy, and the classification rate for the various ECG beat types. The classification results are summarized in Table 4.1 and Table 4.2.

The overall classification rate was 97.52%, which is good compared to those of existing computer-based methods, whose median is 91.3% [56]. In some recordings (203, 222, and 223), the classification rate was rather low. An examination of these recordings indicates a high variation of the length of the RR intervals around normal beats. This variation causes normal beats to be classified as APBs.

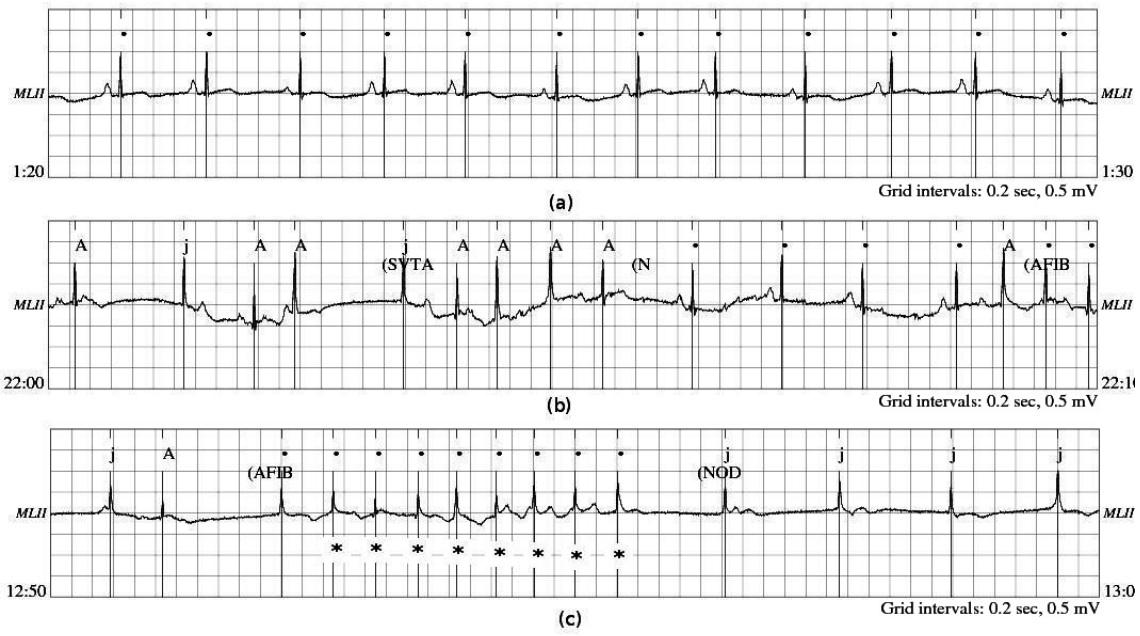

Figure 4.5: Segments of recording 222 from MIT/BIH arrhythmia database (• = NB, A = APB, ∗ = NB classified as APB).

Figure 4.5 shows the irregular heart rate of recording 222. Figure 4.5(a) shows a segment of the first five minutes of recording 222 and an estimate of the mean RR (RR_m), which is a feature used for the discrimination of APBs. The classification rule defined in step (5) works fine for the detection of APBs in figure 4.5(b), but fails in figure 4.5(c) because the classifier identifies NBs as APBs. The same situation occurred for recording 203, as shown in figure 4.6. The error rate in the classification of these recordings can be lowered if the mean RR (RR_m) is calculated from a moving window of some width on the remaining 25

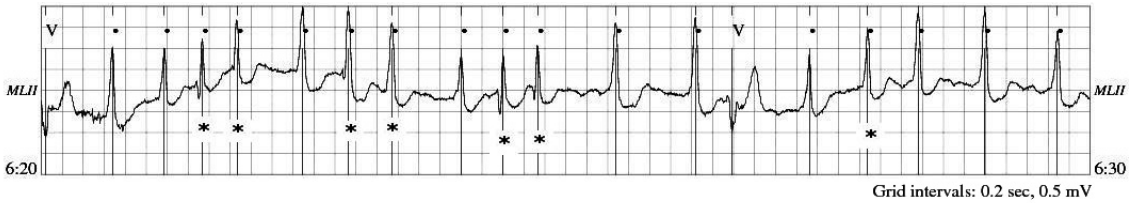

Figure 4.6: Segment of recording 203 from MIT/BIH arrhythmia database (• = NB, v = PVC, ∗ = NB classified as APB).

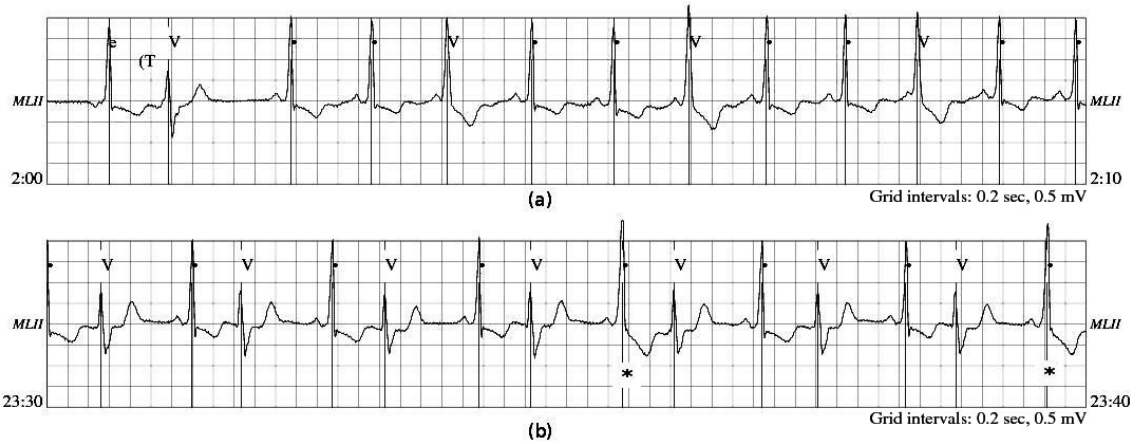

Figure 4.7: Segments of recording 223 from MIT/BIH arrhythmia database (• = NB, v = PVC, ∗ = NB classified as PVC).

minutes of data. For recording 223, some NBs appear similar to PVCs, as shown in figure 4.7. The proposed method incorrectly classifies these beats because the classification for PVCs is only based on the waveform similarity. The classification of PVCs can be improved by taking into account the premature nature and the compensatory pause that characterize PVCs. Misclassification can also result from errors in the position of R peaks provided by the manually annotated files in the MIT-BIH database. The proposed similarity function can give poor results for two beats in a given class if their R peaks are misaligned at the top of their QRS complex. In the proposed method, creating the heart beat database used by the classifier can be difficult. However, as stated in [56], computer-based interpretations of ECG recordings cannot replace those of an electrocardiographer, and all reports obtained using a computer-based method require confirmation by a physician. A comparison of the proposed method to related works is summarized in Table 4.3. An efficiency comparison of methods is not straightforward due to the differences in the test conditions (e.g., types of beat classified and number of beats used for testing).

Some previously reported methods were tested on a relatively small number of beats. For example, for the independent component analysis [15] method, the authors used 25 recording, with at most 300 beats used for training and 300 beats used for testing per record even for those that contained more than 2000 beats. Since the morphology of beats of a given type not only changes from patient to patient but also within a given patient, the number of beats used for testing can impact the recognition accuracy. In Table 4.1, if recordings 203, 222, and 223, which give bad results, are removed, the overall classification rate of the proposed method increases from 97.52% to 98.53%.

4.5 Conclusion

A patient-adaptable ECG beat classification method based on a similarity function and a beat database was presented. The discrete wavelet transform is used for ECG signal preprocessing. The method uses a simple approach and wavelet-based data compression for database storage and low-cost processing. A high classification accuracy was obtained for six types of heart beat.

Table 4.1: Classification results.

Recording number	Number of beats	Number of misclassified beats	Classification rate (%)
100	1892	0	100
101	1514	2	99.87
103	1721	5	99.71
105	2141	71	96.68
106	1688	52	96.92
107	1776	11	99.38
108	1468	53	96.39
109	2089	11	99.47
111	1768	41	97.68
112	2101	2	99.90
113	1498	3	99.80
114	1590	44	97.23
115	1628	1	99.94
116	2007	23	98.85
117	1277	3	99.77
118	1907	42	97.80
119	1653	0	100
121	1551	5	99.68
122	2044	0	100
123	1262	0	100
124	1334	12	99.10
200	2156	76	96.47
201	1408	44	96.88
202	1860	63	96.61
203	2467	592	76
205	2180	6	99.72
207	1475	21	98.58
208	2122	19	99.10
209	2509	109	95.66
210	2164	57	97.37
212	2275	7	99.69
213	2450	40	98.35
214	1866	86	95.39
215	2780	104	96.26
217	1608	12	99.25
219	1764	44	97.51
220	1685	36	97.86
221	2011	2	99.90
222	1892	279	85.25
223	2166	265	87.77
228	1695	29	98.29
230	1849	2	99.89
231	1270	12	99.06
232	1478	16	98.92
233	2543	44	98.27
234	2231	0	100
Average			97.52

Table 4.2: Classification rate per ECG beat type.

Beat type	Number of beats	Number of misclassified beats	Classification rate (%)
NB	61896	638	98.96
PB	2952	6	99.80
LBBB	6856	49	99.29
RBBB	5870	44	99.25
APB	2270	414	81.76
PVC	5969	1195	79.97

Table 4.3: Comparison results of various ECG beat classification methods.

Method	Number of beat types	Accuracy (%)
ICA [15]	6	99.51
FTNN [8]	3	98
MOE [12]	4	94
MRANN [9]	13	96.79
FHNN [1]	7	96.6
Proposed method	6	97.52

Chapter 5

Automated localisation and classification of abnormal beats in electrocardiograms using parsimonious wavelet analysis

5.1 Introduction

Electrocardiogram is a recording of the electric activity on the (chest) skin induced by depolarisation waves of the heart muscle. The frequency of the depolarisation waves for a healthy heart at rest is of the order of 1 Hz (or slightly higher) while the amplitude of the recorded electric pulse is of the order of 1 mV. The normal cycle of the heart has a very idiosyncratic appearance depicted in figure 5.1: the cycle begins by a progressively developing voltage bump known as P wave, a rapid depolarisation-polarisation voltage giving rise to the most prominent feature of the cycle, known as QRS complex, followed by another bump known as T wave. A reliable estimate of the heart frequency is provided by the RR distance of two subsequent QRS complexes.

Although the expertise of the clinician is ultimately necessary to diagnose whether a heart beats normally or not, huge efforts are being deployed towards continuously monitoring the heart activity of patients, detecting abnormal beats, and issuing alerts in case of danger. With the aging of the population living in isolation, it becomes more urgent to have reliable methods of automatically localising abnormal beats on the monitoring records and possibly determining the class of abnormality.

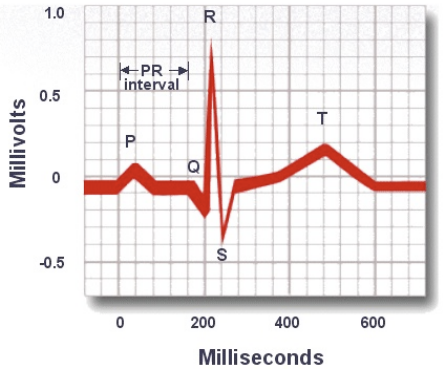

Figure 5.1: Schematic representation of a normal ECG cycle. Observe that the QRS complex appears as the most prominent future.

The main difficulty in automated localisation and classification of abnormal beats stems in the high variability of the electrocardiogram: it is only approximately periodic, some features can be missing or non recognisable within one period, the recorded electric activity can be corrupted by noise, etc.

In this chapter we introduce a parsimonious and computationally efficient method which automatically analyse electrocardiograms with the help of wavelet bases. The method automatically localises points of interest (QRS complexes) and decides whether they are normal or not. We use wavelet basis to decompose the time signal but a different analysis is subsequently performed to extract the most prominent features. The proposed analysis method is computationally very efficient and can ultimately be incorporated as a real time processing unit on the recording device.

In order to test our method, we have used the MIT-BIH arrhythmia data base. This data base contains 48 recordings of electrocardiograms performed on patients with different pathologies. Recordings are discrete versions of the continuous electrophysiological potentials, sampled at a frequency of 360 Hz (i.e. there are 21600 sample points per minute) and run for a total time span of slightly more than 30 minutes (more precisely 650000 sample points per recording). All recordings are fully annotated by two independent physicians; a single letter code is used to design the nature of every beat.

The method presented in this chapter is published in [88].

5.2 QRS detection algorithms

A QRS detector is designed to detect heart beats within ECGs. Heart beat detection is a usefull procedure preceding any kind of ECG processing and analysis (classification, some denoising algorithm, etc.). In this thesis we have used the annotation files of the MIT-Arrhythmia Database for heart beats localization but in practice one must use a QRS detection algorithms.

There exist a large variety of QRS detection algorithms, but none of them proves universally acceptable accuracy. Therefore efforts are constantly deployed for their enhancement. The main difficulty in automatic QRS detection is due to the noise corrupting the electrocardiogram, and sometimes the signal to noise ratio can be very low. Some of these algorithms are cited in [57].

5.3 Analysis

5.3.1 The parsimonious wavelet analysis of ECG signals

Each ECG signal has obviously finite energy, therefore can be considered as an element $f \in L^2(\mathbb{R})$; consequently, the previous analysis holds. Now the signals of the MIT-BIH arrhythmia database come in records of $N = 650000$ points. In view of the aim we fixed in the beginning of providing a computationally very efficient method that could ultimately be incorporated in real time recording devices, we seek a very parsimonious representation of the signal. Since the larger integer J such that $2^J \leq N$ is $J = 19$, we focus on the detail wavelet coefficients $c_{J,k}$. We define the **set of parsimony** by $\Pi_\theta = \{k \in \mathbb{Z} : |c_{J-1,k}| > \theta\}$ for some threshold θ. We use the adjective "parsimonious" to denote the fact of keeping merely coefficients in Π_θ as the only information on the signal[1].

5.3.2 Marking the points of interest

For a fixed integer $w > 0$, we determine the **potentially interesting points** of the ECG by choosing those $k \in \Pi_\theta$ that correspond to a local maximum within the window of width w.

Let $(k_0, k_1, \ldots, k_{L-1})$ be an ordered enumeration of the interesting points (correspond-

[1] Parsimony is not to be confused with the related but distinct notion of "sparsity", i.e. the — non linear — representation of the signal f in terms of its decomposition on those elements of the basis minimising the quadratic error [45].

ing to the time instants $(k_l/2^{J-1})_{l=0,\ldots,L-1}$). A synthetic qualitative way of representing the whole ECG is by plotting the cloud of points $(k_l, k_{l+1} - k_l)_{l=0,\ldots,L-2}$ having as abscissa the time instant of occurrence and as ordinate the difference of the abscissas between the current and the next interesting points. For normal ECG, with frank QRS complexes and cutoff threshold θ set to a sufficiently high value, it is expected that the cloud of points will cluster around a constant level of approximately 300 points because the interesting points will correspond then to the R peak and the distance between two successive R peaks will correspond to the period of the heart cycle. Any deviation from this normal situation must be interpreted as a signature of some abnormality that must be explored; it may concern some physiological abnormality like ectopy, premature beats, fibrillation, paced beats, etc. or technical abnormality like high level of noise due to bad contact of electrodes or interference. Some examples of such synthetic qualitative pictures are provided as left hand side subfigures (labelled a) in figures 5.2, 5.3, 5.4, and 5.5. Note that in these subfigures, the abscissas are in time units of minutes while the ordinates are in time units of sample points (i.e. in units of $\frac{1}{360}$ seconds).

5.3.3 QRS mask and recognition of the shape of the QRS complex

Although the previous marking of interesting points considers relative positions of consecutive events (successive local maxima), in this subsection, we focus on purely local shape recognition. We start by automatically recognising and localising the features of the cycle that are potential candidates for QRS complexes. For every $k \in \Pi_\theta$, and a fixed window width $w > 0$, we apply a $\{0,1\}$-masking function $M_{\text{nqrs}} : \Pi_\theta \to \{0,1\}$ defined on points at the finer resolution. If $M_{\text{nqrs}}(k) = 1$ then the ECG signal around $k/2^{J-1}$ is proposed by our method as a tentative QRS complex. The masking function depends on the used wavelet basis. The results reported here concern the simplest case of Haar wavelets but there is no difficulty to define masking functions for other types of compactly supported wavelets.

More precisely, for the analysis in terms of Haar wavelets, the function M_{nqrs} is determined by the following algorithm.

Require: integer $k \in \mathbb{Z}$;
integer $w > 0$;
set $A = \Pi_\theta \cap [k - w, k + w]$;
sequence $(c_{J-1,l})_{l \in \{k-w,\ldots,k+w\}}$;
real parameters θ_0 and θ_1 with $0 < \theta_1 \leq \theta_0$.
Ensure: M_{nqrs}.
for $m \in A$ **do**
$M_{\text{nqrs}}(m) \leftarrow 0$
$k_0 \leftarrow \arg\max\{c_{J-1,l} : l \in A, |l - k| \leq w\}$

$k_1 \leftarrow \arg\min\{c_{J-1,l} : l \in A, l - k_0 > -w\}$
if $c_{J-1,k_0} > \theta_0 \quad \& \quad c_{J-1,k_1} < -\theta_1$ **then**
$M_{\text{nqrs}}(k_0) \leftarrow 1$
end if
end for

The rationale behind the use of this masking function is summarised as follows. The finest resolution wavelets have a support span of the order of 2^{-J} sample points. Now normal ECG cycles look as in figure 5.1. It turns out that the only wavelet coefficients at this resolution exceeding a threshold of the order $\theta \simeq 0.05$ are those whose support intersects significantly the support of the QRS complex of a normal cycle. Additionally, since the QRS starts by a steep decrease in voltage and continues with an even steeper increase, if we find a (positive) local maximum of c_{J-1,k_1}, preceeded by a negative local minimum c_{J-1,k_0} and $k_1 - k_0$ is small enough (some units), then provides an efficient method to recognise the shape of the QRS complex and localise its position with tremendous accuracy. The parameters θ_0, θ_1 and w needed in the previous algorithm can be determined either *ad hoc*, or by supervised learning on a database.

In the right hand side (labelled b) of the figures 5.2, 5.3, 5.4, and 5.5, we give examples of detailed view around interesting points where our method and MIT annotation disagree. In subfigures b) we plot two graphs: one on the bottom, containing the values of the wavelet coefficients $c_{J-1,k}$ for $k \in \Pi_\theta$ (the other are set to 0); one on the top, containing the experimental ECG recording (vertically rescaled and shifted to hold in the same graph). The time unit of the abscissas of the subgraphs b) is set in seconds. The scale of the ordinates is set and fixed but is irrelevant.

Once the potential QRS complexes are identified, similar masks recognising other shapes like the P or T waves, for instance, can be applied. We postpone their analysis into a subsequent publication.

5.4 Summary of the results

5.4.1 Qualitative localisation of marked points

Analysis of the 48 files give very diverse results. Although we report here on the figures obtained for only 4 different files, we have analysed all 48 cases. Most of the points normally cluster around 300 points (see figures 5.2a, 5.3a, 5.4a, and 5.5a); this cluster corresponds to candidate beats at normal pace. When some points are outside the standard deviation band around the central cluster, they correspond to some local perturbations of the heart rhythm occurring to atrial or ventricular premature beats (we have such examples even in

the normal recording 100 (figure 5.2a), where a few points lie outside a standard deviation from the main cluster. Some graphs exhibit two clusters, one around 300 points and another around 25 points (see figure 5.3a); they are typical of a situation where the heart is stimulated by a pacemaker. Some other graphs scatter all way from 300 down to 0 (see figure 5.4a around the abscissa at 20 minutes and 5.5a around the abscissa 3 minutes); they correspond to noise situations or atrial or ventricular fibrillation.

5.4.2 Shape recognition of the normal QRS complexes

For determining the QRS complexes we have used merely an *ad hoc* fixing of the parameters defining the function M_{nqrs}. The reason of not using supervised learning is that there are some annotations in the MIT-BIH database that we think are inconsistent. We limited the scope of this study in exploring both the advantages and the possible pitfalls of the method; we postpone to a subsequent publication the full fledged analysis after we have reviewed the annotations of the database with the help and expertise of cardiologists.

Using our method we have marked all potentially interesting beats that passed through the QRS *ad hoc* mask function and confront them with all MIT annotated beats and all beats marked by MIT physicians as normal. For the file 100 (healthy patient) we have a good agreement, there are pronounced discrepancies on the other files. On the table 5.1, we regroup the statistics of the shape recognition of potential QRS complexes on all the 48 files of the MIT-BIH arrhythmia database. We provide the reader with tentative explanations of the discrepancies on some specific examples.

5.4.3 Comments on specific files

Several comments are due. First of all, for some files we obtain good agreement, for other the agreement seems very poor. We argue on a small number of files.

File 100

This file corresponds to a patient with (essentially) periodic rhythm[2]. The figure 5.2a is a synoptic view of the file 100. Most points cluster around the ordinate of 300 sample points (or 0.83 s) corresponding to a periodic cardiac rhythm. Now, in the one letter annotation of the MIT database, we have found some inconsistencies since shape characteristics are mixed with rhythm caracteristics.

[2]Periodic rhythm is termed sinusoidal in the cardiological jargon.

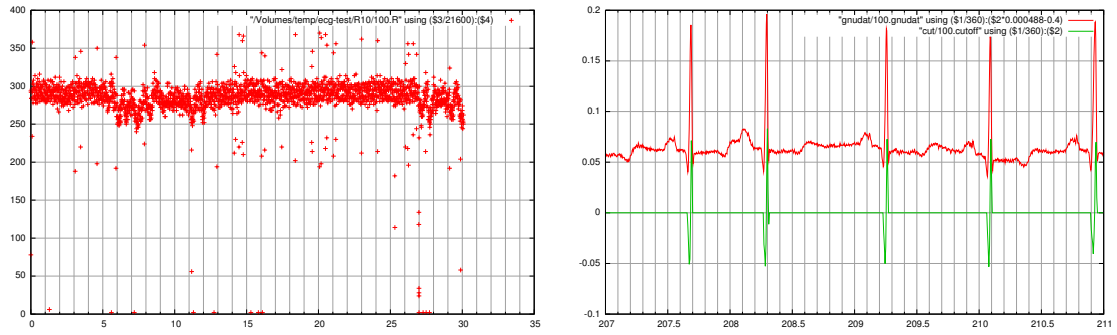

(a) (b)

Figure 5.2: File 100: a) synoptic view, b) details around beat at 208.3 s.

Looking more precisely on the 34 beats that are classified as normal (QRS-shaped) beats by our method while they are annotated as abnormal (code different from N) in the MIT database — hence counted as false positive in the comparison statistics table — have the standard QRS shape. However, they arrive slightly prematurely within the cycle; therefore they are classified as atrial premature beats (code A) in the database. An example of this phenomenon appears in the figure 5.2b depicting the behaviour of the ECG around the beat at 208.3 seconds (or at 74988 sampling points). The beat (on the top level) looks perfectly normal and is detected as such and precisely localised by our method (lower level). The reason of the discrepancy is that the RR distance with the preceding beat is 0.62 s (or 223 sample points) while the distance with the following beat is 1.3 s (or 468 sample points).

File 102

The analysis of this file presents the particularity of detecting no coincidence at all. The figure 5.3a uses the same representation as before. We observe two clustering sets, one at 280 sample points (or 0.78 s) and another at 35 points (or 0.1 s). The situation depicted here corresponds typically to a heart stimulated by a pacemaker.

Remarkably no coincidence is observed in the statistics. The explanation is provided in the figure 5.3b where a detailed view of the ECG and our detection process are depicted. Although the R beat is properly localised by our method and its position coincides with the position annotated by the MIT team, there is no coincidence because the peaks are annotated as abnormal (paced beat). Again, the observed discrepancy is not a weakness of our method but an insufficiently precise annotation of the MIT base where shape and frequency details are merged.

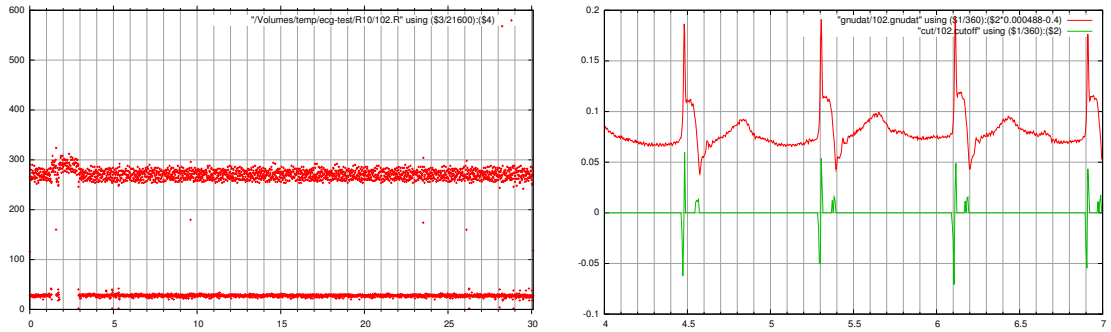

(a) (b)

Figure 5.3: File 102: a) synoptic view, b) details in the inverval [4 s, 7 s].

File 105

The beats of this file are in their great majority annotated as normal QRS complexes (code N) in the MIT basis while they fail to pass the normal QRS mask function in our test. Looking on figure 5.4, we remark two facts. First, the figure 5.4b represents a detailed view of the time span having beats annotated as normal by the MIT team and failing to pass our QRS mask. We remark that the wavelet coefficients (on the lower part of the right figure) are of significantly smaller amplitude than their counterparts in file 100. The reason is that the QRS complex (see upper part of the right figure) is less steep than the corresponding QRS of file 100 and is not preceded by a drop of the voltage after the onset Q.

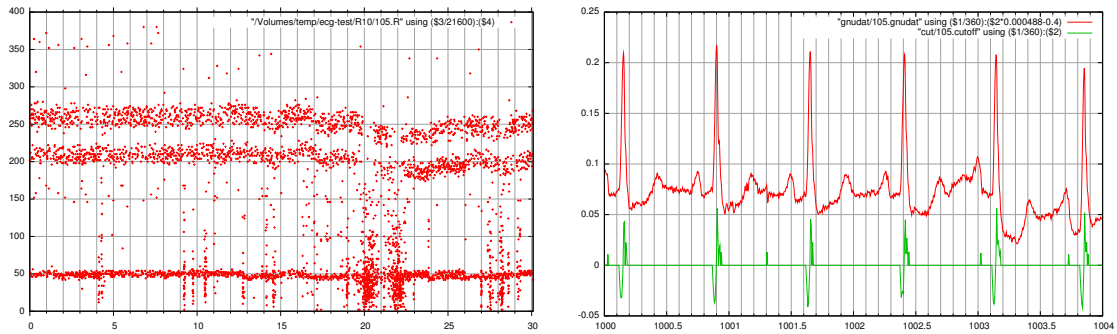

(a) (b)

Figure 5.4: File 105: a) synoptic view, b) details in the inverval [1000s, 1004s].

Secondly, on the synoptic view presented on the figure 5.4a, we detect the presence of three clusters. Contrary to file 100 where the local maxima within the cycle are determined by the frank R peaks, here the P or T waves give similar contributions to the wavelet coefficients. The clustering is around the PR, RR, and RT distances.

File 111

Here both our method and the MIT agree on non detecting any normal beats. The fact that we get 0 coincidence is therefore a successful test of our method for this file. The reasons for this result are visible to both the synoptic view of the ECG and the detailed view (see figure 5.5).

On the detailed view, we remark that the R peaks have a preceding spike; therefore the MIT team annotates the peaks as "left bundle branch block beat" (code L). The presence of the spike makes the onset of the R peak less steep than normal and hence the numerical value of the wavelet coefficient smaller than normal. Therefore, the beats fail to pass through the QRS normality mask.

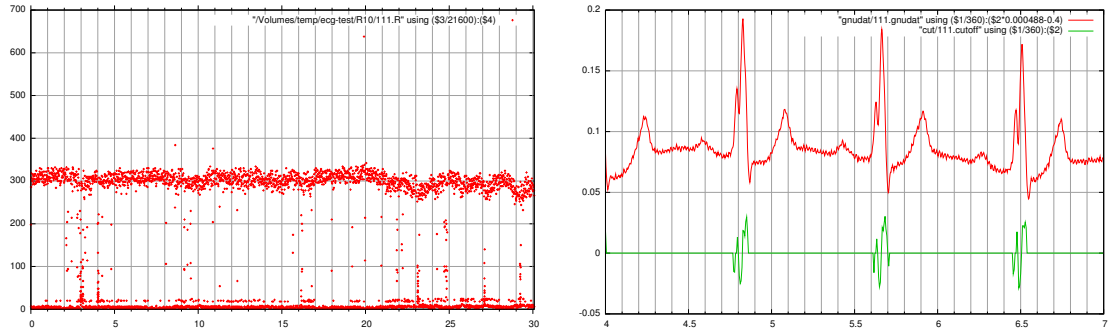

(a) (b)

Figure 5.5: File 111: a) synoptic view, b) details in the inverval [7 s, 11 s].

However, the peaks are sufficiently strong to trigger the function I so that we classify them as potentially interesting. Since the spikes are very close to the R peak, we observe the low lying cluster on the synoptic view.

5.4.4 Computational complexity

The main characteristic of our method is its locality. First, the computation of each wavelet coefficient is performed, locally in time, and in $\mathcal{O}(|\text{supp}|)$ operations, where supp is the support of the compactly supported scaled mother function $\psi(2^{J-1} \cdot -k)$. Secondly, the computation of the functions I and M_{nqrs} is performed in $\mathcal{O}(w)$ operations. In the final version of the method, masks for the other types of beats will be needed. However, there are very few other masks to be determined. Therefore, the overall computational complexity is of constant type. As for space complexity, the needed storage is also very limited. For normal QRS detection, the storage is of the order of $2w$. For more complicated masks, the previous and possibly penultimate location must be stored. Therefore, the space complexity is also of constant type.

5.5 Conclusion

We have introduced a computationally efficient method to localise and classify heart beats. We have analysed all the 48 files of the MIT-BIH arrhythmia database. For all files we have identified the reasons of coincidence or discrepancy and determined the actions we must take in order to have complete agreement. Therefore, from the side of the mathematical analysis of the ECG signal processing, our method is validated and well understood. What is still lacking is the cardiological expertise needed to determine the mask function for assessing normal QRS complexes, P or T waves, noise, fibrillation, premature atrial or ventricular events, etc. a process that is in progress.

File identifier	Our normal	MIT marked	MIT normal	Coincidences	False positive	False negative
100	2274	2237	2203	2202	34	0
101	1853	1840	1826	1812	6	13
102	1694	2156	99	0	9	98
103	2256	2057	2048	2047	169	0
104	2281	2272	163	101	2005	61
105	730	2650	2487	652	75	1822
106	1741	2063	1473	1405	298	67
107	462	2104	0	0	0	0
108	70	1791	1710	63	5	1455
109	1133	2488	0	0	0	0
111	3	2098	0	0	0	0
112	177	2507	2494	175	1	2215
113	1795	1767	1761	1760	5	0
114	913	1863	1793	873	34	919
115	1953	1931	1922	1921	0	0
116	2395	2382	2263	2242	112	20
117	1434	1514	1509	1392	16	116
118	2332	2264	0	0	0	0
119	1544	2061	1519	1518	0	0
121	0	1846	1831	0	0	0
122	2474	2434	2431	2428	0	2
123	1515	1495	1491	1490	0	0
124	1804	1609	0	0	0	0
200	1552	2747	1715	1337	184	373
201	535	1995	1581	496	17	1082
202	1638	2120	2036	1593	36	442
203	1449	3055	2482	1136	254	1325
205	2541	2628	2527	2482	14	44
207	41	2356	0	0	0	0
208	1953	2986	1561	1540	380	20
209	3048	3006	2575	2573	428	1
210	1458	2639	2381	1423	29	957
212	2788	2718	923	922	1770	0
213	3126	3239	2586	2584	486	1
214	2142	2298	0	0	0	0
215	3378	3344	3144	3128	194	15
217	1079	2244	244	243	501	0
219	2122	2276	2046	2042	43	3
220	2048	2033	1918	1917	94	0
221	2013	2424	1999	1964	16	34
222	1601	2596	2024	1292	293	731
223	2023	2603	1990	1817	165	172
228	312	2100	1659	22	280	1629
230	2263	2422	2214	2213	8	0
231	1565	1979	314	313	1105	0
232	1312	1787	0	0	0	0
233	2577	3099	2195	2164	365	30
234	2740	2718	2654	2642	51	11

Table 5.1: Normal beats detection statistics on the 48 MIT files.

Chapter 6

Conclusion and future work

This thesis focused on the analysis of electrocardiograms in view to develop new effective methods of classification of arrhythmias (a diagnostic tool) and localization and automatic detection of abnormal heart beats in real time ECG signal (a monitoring tool).

The electrocardiogram is a valuable tool for studying the electrical activity of the heart. Therefore medical and technical basics necessary for the understanding of ECG signal are provided in chapter 2. ECG lead systems and normal heart beats and different arrhythmias as well as heartbeat morphologies are described in that chapter.

Chapter 3 is dedicated to mathematical tools for signal processing with wavelet transform. ECG signal preprocessing techniques for low-frequency and high-frequency noise cancellation based on wavelet transform have been implemented. Wavelet data compression have also been carried out for length reduction of extracted heart beats before analysis. This data compression is usefull for database storage and low-cost processing.

Chapter 4 and 5 gives actual implemention of techniques presented in previous chapters and details on methods proposed in this thesis. The heart beats classification method is patient-adaptable and is based on a similarity function and experience-based rules. The localization method is of very low time and space computational complexity because it uses only one part of the avaivable datas (a set of parsimony). It is based on a mask function for assessing normal QRS complexes. Both methods are evaluated on ECG signals of the MIT-BIH arrhythmia database. This database contains 48 half-hour excerpts of two-channel ambulatory ECG recordings (annotated and digitized at 360 samples per second), obtained from 47 subjects. The proposed classification and localization methods gives respectively high classification accuracy and tremendous localization accuracy.

Nevertheless, some future work can improve these methods:

- Some little difficulty in the application of the classification method can be the creation of the heart beats database. A solution to circumvent this difficulty would be to reduce the redundancy in the first five minutes of the ECG recording to annotate manually for integration into the heart beat database.
- Add patches to better identify APB and PVC beats.
- Expand the scope of the classification method to other types of arrhythmias.
- For the localisation method, parameters θ_0, θ_1 and w can be better estimated using a part of the signal.
- Define other masking functions for le localisation of P and T waves needed to better detect abnormal QRS.

Bibliography

[1] S. Osowski and T. H. Linh, "ECG beat recognition using fuzzy hybrid neural network," *IEEE T. Bio-Med. Eng.*, 48: 1265-1271, 2001.

[2] S. Osowski, T. Markiewicz and L. Tran Hoai, "Recognition and classification system of arrhythmia using ensemble of neural networks," *Measurement*, 41: 610-617, 2008.

[3] L. Shyu, W. Hu, "Intelligent Hybrid Methods for ECG Classification-A Review," Journal of Medical and Biological Engineering, 28(1): 1-10 (2007).

[4] J. Malmivuo, R. Plonsey "Bioelectromagnetism - Principles and Applications of Bioelectric and Biomagnetic Fields", New York Oxford University Press (1995).

[5] A. Welinder, L. Sörnmo, D. Q. Feild, C. L. Feldman, J. Pettersson, G. S. Wagner, O. Pahlm "Comparison of signal quality between easi and mason-likar 12-lead electrocardiograms during physical activity," American journal of critical care, May 2004, Volume 13, No. 3.

[6] B. U. Kohler, C. Hennig and R. Orglmeister, "The principles of software QRS detection," *IEEE Eng. Med. Biol.*, 21: 42-57, 2002.

[7] R. Acharya, A. Kumar, P. Bhat, C. Lim, S. lyengar, N. Kannathal and S. Krishnan, "Classification of cardiac abnormalities using heart rate signals," *Med. Biol. Eng. Comput.*, 42: 288-293, 2004.

[8] K. Minami, H. Nakajima and T. Toyoshima, "Real-time discrimination of ventricular tachyarrhythmia with Fourier-transform neural network," *IEEE T. Bio-Med. Eng.*, 46: 179-185, 1999.

[9] G. K. Prasad and J. S. Sahambi, "Classification of ECG arrhythmias using multi-resolution analysis and neural networks," *IEEE Conf. on Convergent Technologies*, 1: 227-231, 2003.

[10] P. C. Ivanov, Q. D. Y. Ma, R. P. Bartsch, J. M. Hausdorff, L. A. N. Amaral, V. Schulte-Frohlinde, H. E. Stanley and M. Yoneyama, "Levels of complexity in scale-invariant neural signals," *Phys. Rev. E*, 79: 041920-041932, 2009.

[11] L. Senhadji, G. Carrault, J. J. Bellanger and G. Passariello, "Comparing Wavelet Transforms for Recognizing Cardiac Patterns," *IEEE Eng. Med. Biol.*, 14: 167-173, 1995.

[12] Y. H. Hu, S. Palreddy and W. J. Tompkins, "A Patient-adaptable ECG beat classifier using a mixture of experts approach," *IEEE T. Bio-Med. Eng.*, 44: 891-900, 1997.

[13] P. De Chazal and R. B. Reilly, "Automatic classification of ECG beats using waveform shape and heart beat interval features," *Int. Conf. Acoust. Spee.*, 2: 269-272, 2003.

[14] Y. Özbay, R. Ceylan and B. Karlik, "A fuzzy clustering neural network architecture for classification of ECG arrhythmias," *Comput. Biol. Med.*, 36: 376-388, 2006.

[15] S. Yu and K. Chou, "A switchable scheme for ECG beat classification based on independent component analysis," *Expert Syst. Appl.*, 33: 824-829, 2007.

[16] M. Engin, "ECG beat classification using neuro-fuzzy network," *Pattern Recogn. Lett.*, 25: 1715-1722, 2004.

[17] Ahmad Khoureich Ka. "ECG beat classification using waveform similarity and RR intervals", Journal of Medical and Biological Engineering, (2011) doi: 10.5405/jmbe.905

[18] "http://www.merckmanuals.com/professional/cardiovascular_disorders/cardiovascular_tests_and_procedures/electrocardiography_ecg.html"

[19] "http://upload.wikimedia.org/wikipedia/commons/b/bd/12leadECG.jpg".

[20] "http://fr.wikipedia.org/wiki/Fichier:ECG_12derivations.png".

[21] "http://en.wikipedia.org/wiki/File:SinusRhythmLabels.svg".

[22] F. G. Yanowitz, "The Alan E. Lindsay ECG tutorial V6.0", University of Utah School of Medicine (July 2007).

[23] "http://www.physionet.org/physiobank/database/mitdb/".

[24] Arialdi M. Miniño, Melonie P. Heron, Sherry L. Murphy, and Kenneth D. Kochanek, "Deaths: Final Data for 2004", National Vital Statistics Reports, Vol. 55, No. 19, August 21, 2007.

[25] "British Heart Foundation Statistics Database www.heartstats.org".

[26] L. Julian Haywood, "Left Bundle Branch Block in Acute Myocardial Infarction: Benign or Malignant?", Journal of the American College of Cardiology, Vol. 46, No. 1, 2005.

[27] M. Gertsch, "The ECG Manual: An Evidence-Based Approach", Springer-Verlag London Limited 2009.

[28] "http://www.americanheart.org".

[29] "http://faculty.unlv.edu/payettea/Biol197/".

[30] M Sami, H Kraemer, DC Harrison, N Houston, C Shimasaki and RF DeBusk, "A new method for evaluating antiarrhythmic drug efficacy", Journal of The American Heart Association, Circulation 1980;62;1172-1179.

[31] Richard J. Harper, William J. Brady, Andrew D. Perron, and Michael Mangrum, "The Paced Electrocardiogram: Issues for the Emergency Physician", American Journal of Emergency Medicine, Volume 19, Number 7, November 2001.

[32] S. Thanigaraj, R. E. Kleiger, "Morphology of right ventricular paced beats in posterior myocardial infarction", Southern medical journal ISSN 0038-4348 2000, vol. 93, no3, pp. 323-326.

[33] George Bachman, Lawrence Narici, and Edward Beckenstein. *Fourier and wavelet analysis*. Universitext. Springer-Verlag, New York, 2000.

[34] Shannon. Communication in the presence of noise. *Proc. I.R.E. [stat/shannon]*, 37:10–21, 1949.

[35] Five short stories about the cardinal series. *Bull. Amer. Math. Soc. (N.S.) [stat/cardinal-series]*, 12(1):45–89, 1985. Available from: http://dx.doi.org/10.1090/S0273-0979-1985-15293-0, doi:10.1090/S0273-0979-1985-15293-0.

[36] Vladimir Aleksandrovich Kotelnikov. On the transmission capacity of the 'ether" and of cables in electrical communications. In *Proceedings of the first all-Union conference on the technological reconstruction of the commu- nications sector and the development of low-current engineering. Moscow [stat/kotelnikov]*, 1933.

[37] Gensun Fang. Whittaker-Kotelnikov-Shannon sampling theorem and aliasing error. *J. Approx. Theory [stat/sampling]*, 85(2):115–131, 1996. Available from: http://dx.doi.org/10.1006/jath.1996.0033, doi:10.1006/jath.1996.0033.

[38] Palle E. T. Jorgensen. *Analysis and probability*: wavelets, signals, fractals, volume 234 of *Graduate Texts in Mathematics*. Springer, New York, 2006.

[39] Alfred Haar. Zur Theorie der orthogonalen Funktionensysteme. *Math. Ann. [wavelets/Haar2]*, 69(3):331–371, 1910. Available from: http://dx.doi.org/10.1007/BF01456326, doi:10.1007/BF01456326.

[40] Alfred Haar. Zur Theorie der orthogonalen Funktionensysteme. *Math. Ann. [wavelets/Haar2]*, 71(1):38–53, 1911. Available from: http://dx.doi.org/10.1007/BF01456927, doi:10.1007/BF01456927.

[41] Alfred Haar. Über asymptotische Entwicklungen von Funktionen. *Math. Ann. [wavelets/Haar3]*, 96(1):69–107, 1927. Available from: http://dx.doi.org/10.1007/BF01209154, doi:10.1007/BF01209154.

[42] Yves Meyer. *Ondelettes et opérateurs. I.* Actualités Mathématiques. [Current Mathematical Topics]. Hermann, Paris, 1990. Ondelettes. [Wavelets].

[43] Yves Meyer. *Ondelettes et opérateurs. II.* Actualités Mathématiques. [Current Mathematical Topics]. Hermann, Paris, 1990. Opérateurs de Calderón-Zygmund. [Calderón-Zygmund operators].

[44] Yves Meyer and R. R. Coifman. *Ondelettes et opérateurs. III.* Actualités Mathématiques. [Current Mathematical Topics]. Hermann, Paris, 1991. Opérateurs multilinéaires. [Multilinear operators].

[45] [wavelets/Mallat2009-WaveletsSparseWay] Mallat. *A wavelet tour of signal processing*. Elsevier/Academic Press, Amsterdam, third edition, 2009. The sparse way,With contributions from Gabriel Peyré.

[46] Ingrid Daubechies. *Ten lectures on wavelets*, volume 61 of *CBMS-NSF Regional Conference Series in Applied Mathematics*. Society for Industrial and Applied Mathematics (SIAM), Philadelphia, PA, 1992.

[47] Ingrid Daubechies, A. Grossmann, and Y. Meyer. Painless nonorthogonal expansions. *J. Math. Phys. [wavelets/DaubechiesMeyer]*, 27(5):1271–1283, 1986. Available from: http://dx.doi.org/10.1063/1.527388, doi:10.1063/1.527388.

[48] Nadine E. Miner, *An Introduction to Wavelet Theory and Analysis*. (1998) Sandia National Laboratories P. 0. Box 5800 Albuquerque, NM 87185-1008.

[49] S. Mallat, "A theory for multiresolution signal decomposition: the wavelet representation," IEEE Pattern Analysis. and Machine Intelligence, 1989, vol. 11, no. 7, pp.674-693.

[50] S. Mallat, "Multiresolution approximations and wavelet orthonormal bases of Ł$_2(\mathbb{R})$", Transaction of the american mathematical society, Volume 315, Number 1, September 1989.

[51] T. Sierocinski, *Méthodes probabilistes, floues et quantiques pour l'extraction de l'information biologique,* Université de Rennes 1 IRMAR, 2008.

[52] Jinsong Tan, kok Seng Chua, Louxin Zhang, and Song Zhu. Algorithmic and complexity issues of three clustering methods in microarray data analysis. *Algorithmica*, 48(2):203-219, 2007. 35.

[53] Roger A. Horn and Charles R. Johnson. Topics in matrix analysis. Cambridge University Press, Cambridge, 1994. Corrected reprint of the 1991 original.

[54] K. Pearson. On lines and planes of closest fit to systems of points in space. Philosophical Magazine, 2:559–572, 1901.

[55] A. H. Kadish, "ACC/AHA clinical competence statement on electrocardiography and ambulatory electrocardiography," *J. Am. Coll. Cardiol.*, 104: 3169-3178, 2001.

[56] P. Kligfield, L. S. Gettes, J. J. Bailey, R. Childers, B. J. Deal, E. W. Hancock, G. van Herpen, J. A. Kors, P. Macfarlane, D. M. Mirvis, O. Pahlm, P. Rautaharju and G. S. Wagner, "Recommendations for the standardization and interpretation of the electrocardiogram: Part I: The electrocardiogram and its technology: A Scientific Statement from the American Heart Association Electrocardiography and Arrhythmias Committee, Council on Clinical Cardiology; the American College of Cardiology Foundation; and the Heart Rhythm Society. Endorsed by the International Society for Computerized Electrocardiology," *Heart Rhythm*, 4: 394-412, 2007.

[57] I. I. Christov, "Real time electrocardiogram QRS detection using combined adaptive threshold," BioMedical Engineering, 2004, 3:28 doi:10.1186/1475-925X-3-28.

[58] Harold Hotelling. New light on the correlation coefficient and its transforms. J. Roy. Statist. Soc. Ser. B., 15:193–225; discussion, 225–232, 1953.

[59] Maurice G. Kendall and Alan Stuart. The advanced theory of statistics. Vol. 2. Hafner Publishing Co., New York, third edition, 1973. Inference and relationship.

[60] Wolfgang Härdle and Léopold Simar. Applied multivariate statistical analysis. Springer, Berlin, second edition, 2007.

[61] Kari Karhunen. Zur Spektraltheorie stochastischer Prozesse. Ann. Acad. Sci. Fennicae. Ser. A. I. Math.-Phys., 1946(34):7, 1946.

[62] Michel Loève. Fonctions aléatoires à décomposition orthogonale exponentielle. Revue Sci., 84:159–162, 1946.

[63] Nelson Dunford and Jacob T. Schwartz. Linear operators. Part I. Wiley Classics Library. John Wiley & Sons Inc., New York, 1988. General theory, With the assistance

of William G. Bade and Robert G. Bartle, Reprint of the 1958 original, A Wiley-Interscience Publication.

[64] N.V. Thakor, Y.S. Zhu, "Applications of adaptive filtering to ECG analysis: noise cancellation and arrhythmia detection", IEEE Trans. Biomed. Eng. 38 (8) (August 1991) 785-794.

[65] E.R. Ferrara, B. Widrow, "The time-sequenced adaptive filter", IEEE Trans. Acoust. Speech Signal Process. 29 (3) (June 1981) 679-683.

[66] V. Almenar, A. Albiol, "A new adaptive scheme for ECG enhancement", Signal Processing 75 (1999) 253-263.

[67] H. SadAbadia, M. Ghasemia, A. Ghaffaria, "A mathematical algorithm for ECG signal denoising using window analysis", Biomed Pap Med Fac Univ Palacky Olomouc Czech Repub. 2007, 151(1):73-78.

[68] M. Alfaouri, K. Daqrouq, "ECG Signal Denoising By Wavelet Transform Thresholding", American Journal of Applied Sciences 5 (3): 276-281, 2008.

[69] B. N. Singh a, A. K. Tiwari, "Optimal selection of wavelet basis function applied to ECG signal denoising", Digital Signal Processing 16 (2006) 275–287.

[70] H.G.Rodney Tan, K.M.Lum and V.H.Mok, "Performance Evaluation of Coifman Wavelet for ECG Signal Denoising", Biomed 06, IFMBE Proceedings 15, pp. 419-422, 2007.

[71] M. Kania, M. Fereniec, R. Maniewski, "Wavelet Denoising for Multi-lead High Resolution ECG Signals", Measurement Science Review, Volume 7, Section 2, No. 4, 2007.

[72] J.A. van Alste, W. van Eck, O.E. Herrmann, ECG baseline wander reduction using linear phase filters, Comput. Biomed. Res. 19 (1986) 417–427.

[73] P. Laguna, R. Jane, P. Caminal, Adaptive filtering of ECG baseline wander, Proceedings of International Conference of the IEEE Engineering in Medical and Biol Medical Society, 1992, pp. 508–509.

[74] A. Khawaja. Thesis: "Automatic ECG Analysis using Principal Component Analysis and Wavelet Transformation," Vol. 3 Karlsruhe Transactions on Biomedical Engeneering (2007).

[75] D. Donoho, I. Johnstone, "Adapting to unknown smoothness via wavelet shrinkage," J.ASA, 1995, vol. 90, pp. 1200-1223.

[76] 2. Friesen GM, Jannett TC, Jadallah MA, Yates SL, Quint SR, Nagle HT "A comparison of the noise sensitivity of nine QRS detection algorithms", IEEE Trans on Biomed Eng 1990, 37:85-98.

[77] R. Poli, S. Cagnoni, G. Valli, "Generic design of optimum linear and nonlinear QRS detection", IEEE Trans on Biomed Eng 1995, 42:1137-1141.

[78] V. X. Afonso, W. J. Tompkins, T. Q. Nguyen, and S. Luo, "ECG beat detection using filter banks". IEEE Transactions on Biomedical Engineering, (1999) 46(2), 192–202.

[79] I. Dotsinsky, T. Stoyanov, "Ventricular beat detection in single channel electrocardiograms", BioMed Eng OnLine 2004, 3:3

[80] Moreas J., Seixas M., Vilani F., Costa E., "A QRS complex detection algorithm using electrocardiogram leads" Comp in Card 2002, 29:205-208.

[81] Englese W., Zeelenberg C., "A single scan algorithm for QRS detection and feature extraction", IEEE Comp in Card 1979:37-42.

[82] Ligtenberg A, Kunt M, "A robust-digital QRS detection algorithm for arrhythmia monitoring", Computers and Biomed Res 1983, 16:273-286.

[83] Li C, Zheng C, Tai C, "Detection of ECG characteristic points using wavelet transforms" IEEE Trans on Biomed Eng 1995, 42:21-28.

[84] A. Gutierrez, P. Hernandez, M. Lara, and S. Perez, "A QRS detection algorithm based on haar wavelet", in Computers in Cardiology 1998, (Cleveland, OH, USA), pp. 353–356, 1998.

[85] Francisco Castells, Pablo Laguna, Leif Sörnmo, Andreas Bollmann, and José Millet Roig. "Principal component analysis in ecg signal processing." EURASIP J. Appl. Signal Process. [ecg/ecg13], 2007:98–98, January 2007. Available from: http://dx.doi.org/10.1155/2007/74580, doi:http://dx.doi.org/10.1155/2007/74580.

[86] L. van der Maaten, E. Postma, J. van den Herik, "Dimensionality Reduction: A Comparative Review," Tilburg centre for Creative Computing, Tilburg University, 2009.

[87] A. K. Ka, "ECG beat classification using waveform similarity and RR intervals", Journal of Medical and Biological Engineering, (2011) doi: 10.5405/jmbe.905.

[88] A. K. Ka and D. Pétritis, "Automated localisation and classification of abnormal beats in electrocardiograms using parsimonious wavelet analysis", ISABEL '11: Proceedings of the 4th International Symposium on Applied Sciences in Biomedical and Communication Technologies, (2011) doi:10.1145/2093698.2093811.

Résumé

Cette thèse a porté sur l'analyse des électrocardiogrammes en vu de développer de nouvelles méthodes efficaces de classification des arythmies (un outil de diagnostique) et de localisation automatique des battements anormaux en temps réel dans un signal ECG (un outil de surveillance). Les signaux ECG sont prétraités et les battements extraits sont compressés puis analysés à l'aide de la décomposition en ondellettes. La méthode de classification proposée exploite les spécificités du patient en faisant un regroupement contextuel des battements et en utilisant une base de données de battements cardiaques annotés. La méthode utilise également une fonction de similarité pour comparer deux battements donnés. La méthode de localisation exploite aussi la décomposition en ondelettes mais se base sur une partie des données disponibles (set of parsimony) pour détecter automatiquement et temps réel à l'aide d'une fonction masque les battements cardiaques anormaux contenus dans le signal ECG. Les deux méthodes ont été testées sur les signaux électrocardiogrammes du MIT-BIH arrhythmia database et des bons résultats ont été obtenus.

Abstract

This thesis focused on the analysis of electrocardiograms in view of developing new effective methods of classification of arrhythmias (a diagnostic tool) and automatic localisation of abnormal beats (monitoring tool) in real time in an ECG signal. The ECG signals are preprocessed and the extracted beats are compressed and then analysed using wavelet transform. The proposed classification method exploits specificities of the patient by doing a contextuel clustering of beats and using a database of annotated heart beats. The method uses also a similarity function to compare two given beats. The localisation method also uses the wavelet decomposition but operates only on a portion of available data (set of parsimony) to automatically detect in real time abnormal heart beats with the aid of a mask function. Both methods were tested on ECG signals from MIT-BIH arrhythmia database and good results have been obtained.